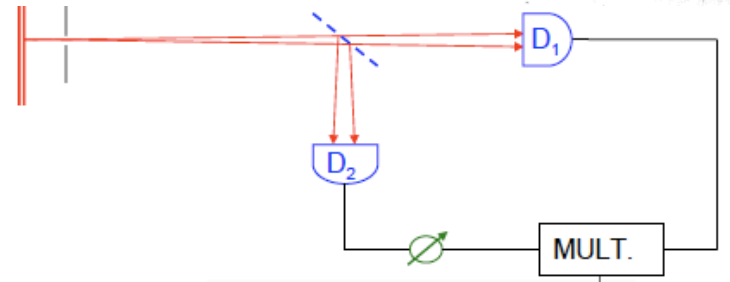


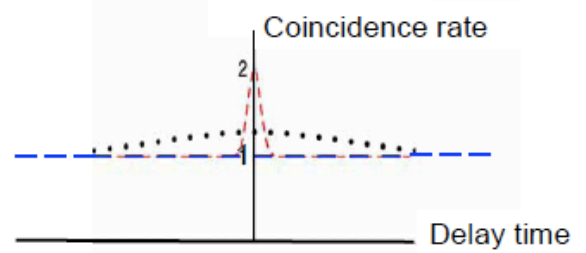
By R. HANBURY BROWN
 University of Manchester, Jodrell Bank Experimental Station

AND

R. Q. TWISS
 Services Electronics Research Laboratory, Baldock



Pound and Rebka '57



Distinguishable:

$$\begin{aligned}
 & \left| \begin{array}{c} \text{---} \\ \text{---} \end{array} \right|^2 + \left| \begin{array}{c} \text{---} \\ \text{---} \end{array} \right|^2 \\
 &= \left| a^2 \right|^2 + \left| a^2 \right|^2 \\
 &= 2a^2
 \end{aligned}$$

$$g^{(2)}(\tau) \equiv \frac{G^{(2)}(\tau)}{|G^{(1)}(0)|^2}$$

$$\begin{aligned}
 G^{(2)}(\tau) &= G^{(2)}(x_2 - x_1) = G^{(2)}(x_1, x_2) \\
 &\equiv \langle E^{(-)}(x_1)E^{(-)}(x_2)E^{(+)}(x_2)E^{(-)}(x_1) \rangle \\
 &\propto \langle a_1^\dagger a_2^\dagger a_2 a_1 \rangle
 \end{aligned}$$

Classical : $g^{(2)}(0) \geq g^{(2)}(\tau)$

Thermal : $g^{(2)}(0) = 2$

Coherent : $g^{(2)}(0) = 1$

Fock $|n\rangle$: $g^{(2)}(0) = 1 - \frac{1}{n}$

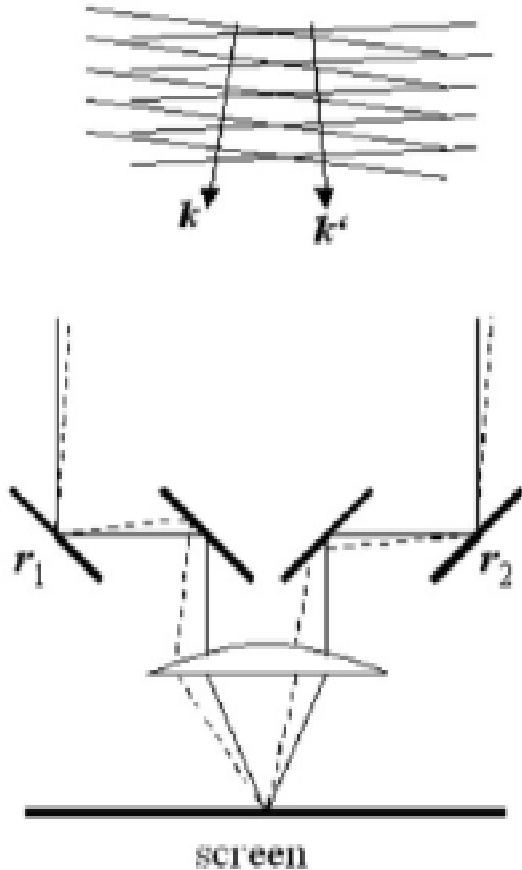
Indistinguishable:

$$\begin{aligned}
 & \left| \begin{array}{c} \text{---} \\ \text{---} \end{array} \right|^2 + \left| \begin{array}{c} \text{---} \\ \text{---} \end{array} \right|^2 \\
 &= \left| a^2 \right|^2 + \left| a^2 \right|^2 \\
 &= 4a^2
 \end{aligned}$$

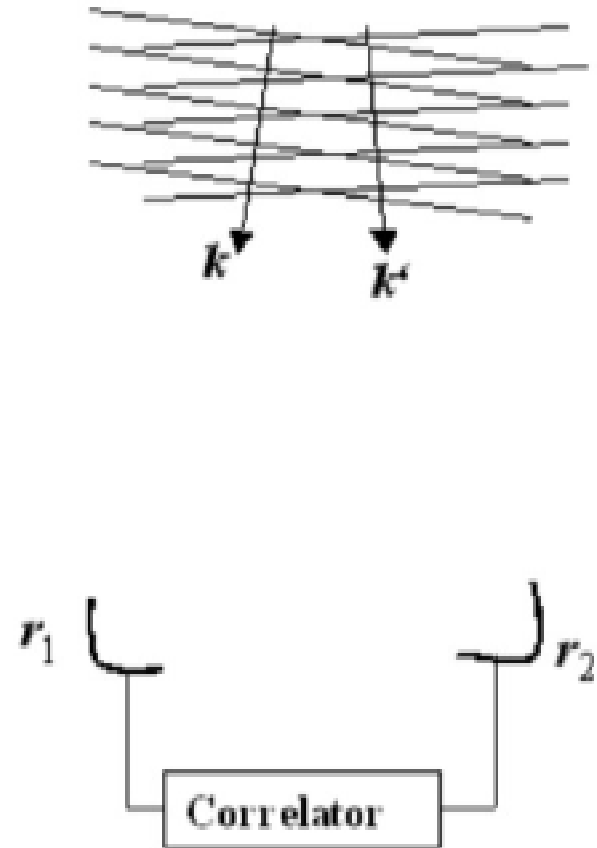
Factor of 2 enhancement due to quantum interference

Hanbury-Brown and Twiss

“Michelson Stellar Interferometry” --
Measure field-field correlations



“HBT Interferometry” --
Measure intensity-intensity correlations

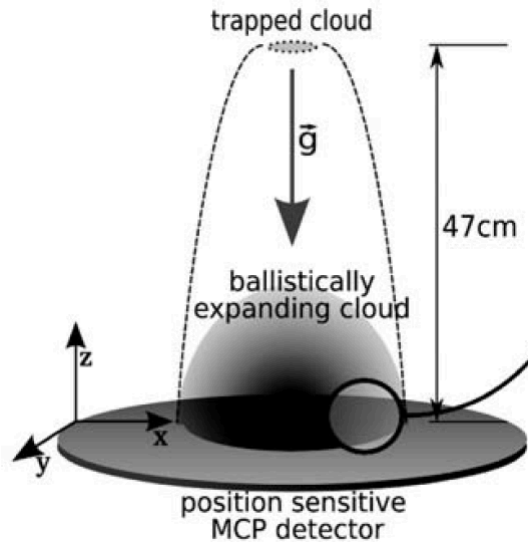


Hanbury Brown Twiss Effect for Ultracold Quantum Gases

M. Schellekens,¹ R. Hoppeler,¹ A. Perrin,¹ J. Viana Gomes,^{1,2}
D. Boiron,¹ A. Aspect,¹ C. I. Westbrook^{1*}

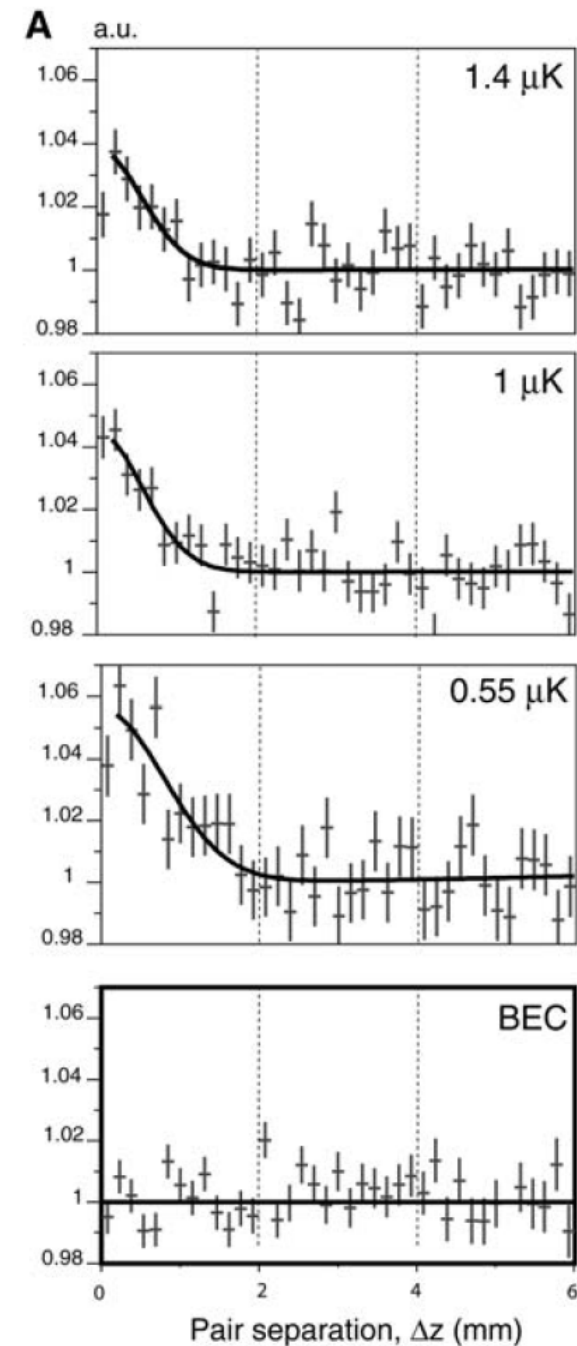
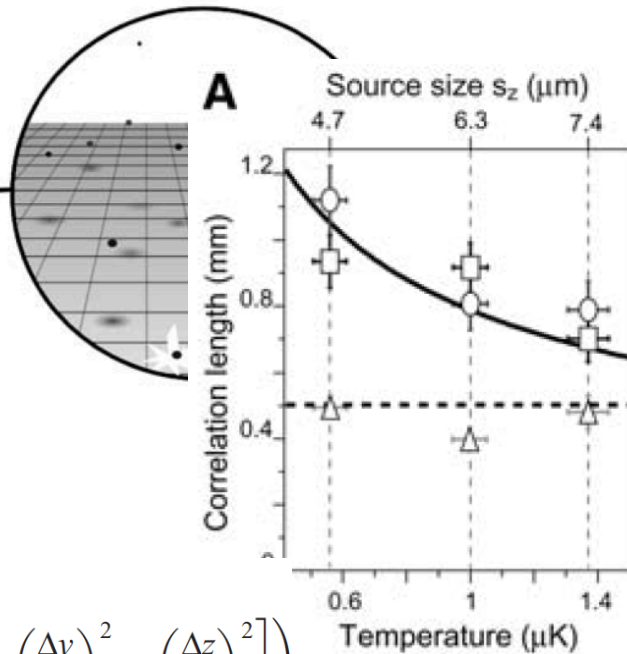
We have studied two-body correlations of atoms in an expanding cloud above and below the Bose-Einstein condensation threshold. The observed correlation function for a thermal cloud shows a bunching behavior, whereas the correlation is flat for a coherent sample. These quantum correlations are the atomic analog of the Hanbury Brown Twiss effect. We observed the effect in three dimensions and studied its dependence on cloud size.

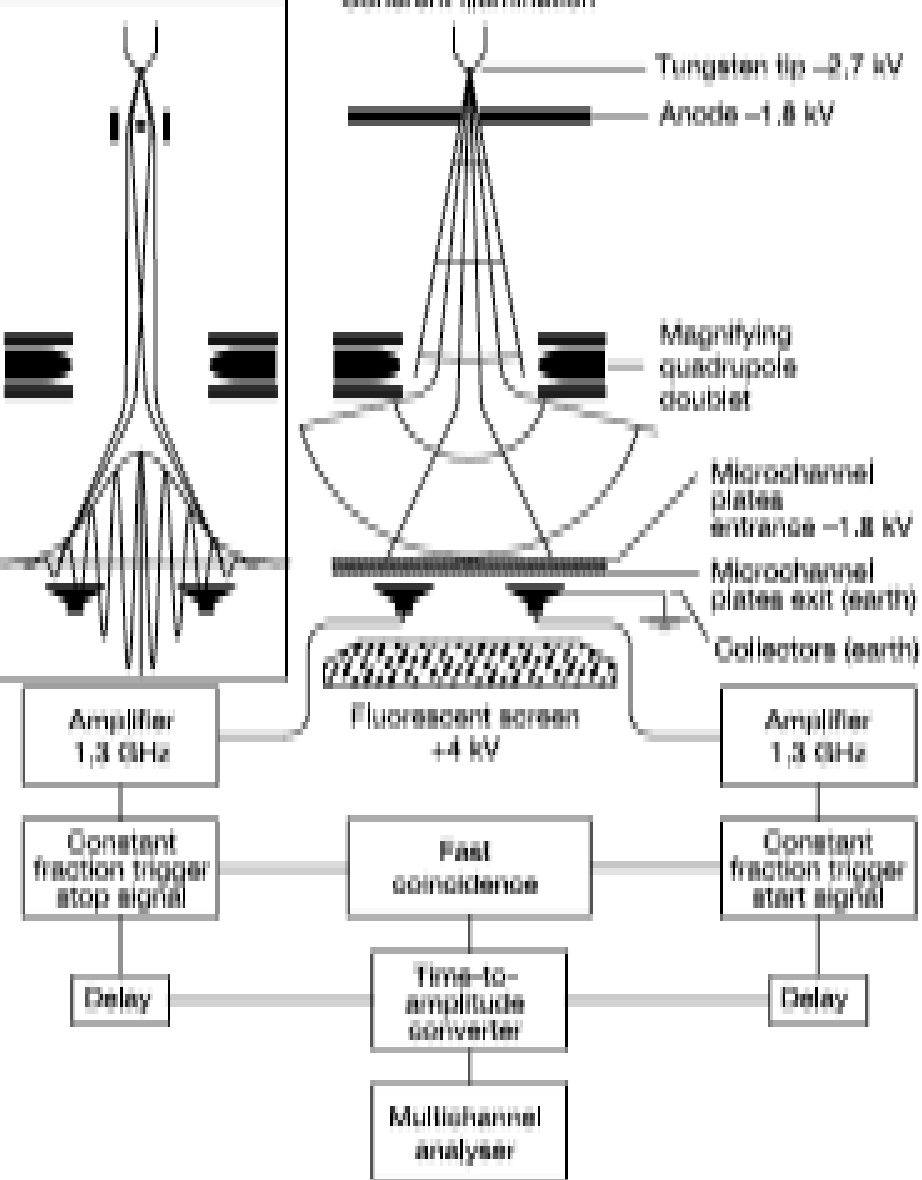
648 28 OCTOBER 2005 VOL 310 SCIENCE



Evaporatively cooled metastable He (which one??)

$$g_{\text{th}}^{(2)}(\Delta x, \Delta y, \Delta z) = 1 + \eta \exp\left(-\left[\left(\frac{\Delta x}{l_x}\right)^2 + \left(\frac{\Delta y}{l_y}\right)^2 + \left(\frac{\Delta z}{l_z}\right)^2\right]\right)$$



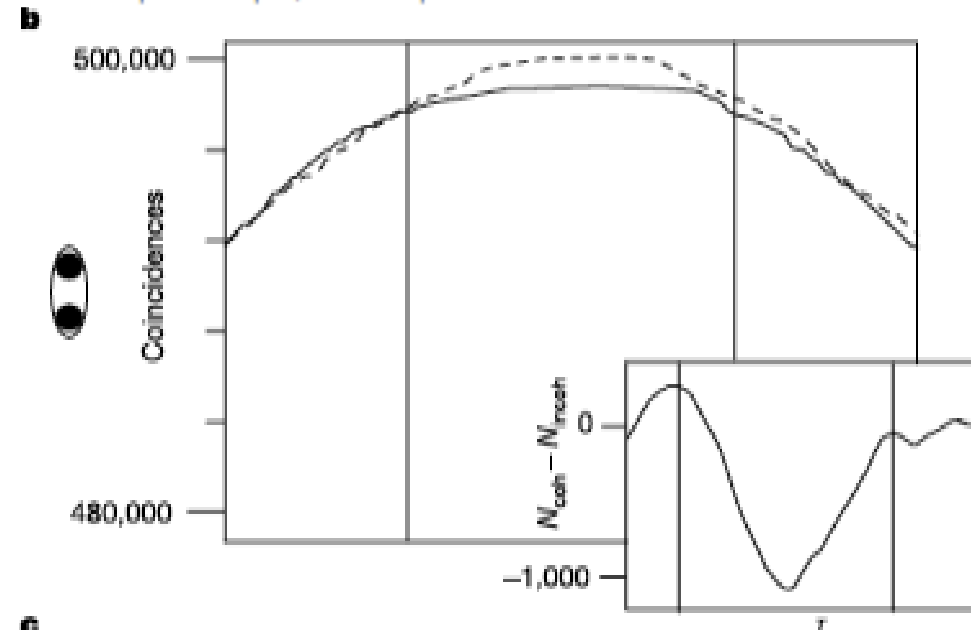


Observation of Hanbury Brown-Twiss anticorrelations for free electrons

Harald Kiesel, Andreas Renz & Franz Hasselbach

NATURE | VOL 418 | 25 JULY 2002 |

392



Experiment with free electrons

Electron correlation time $\sim 10^{-14}$ s

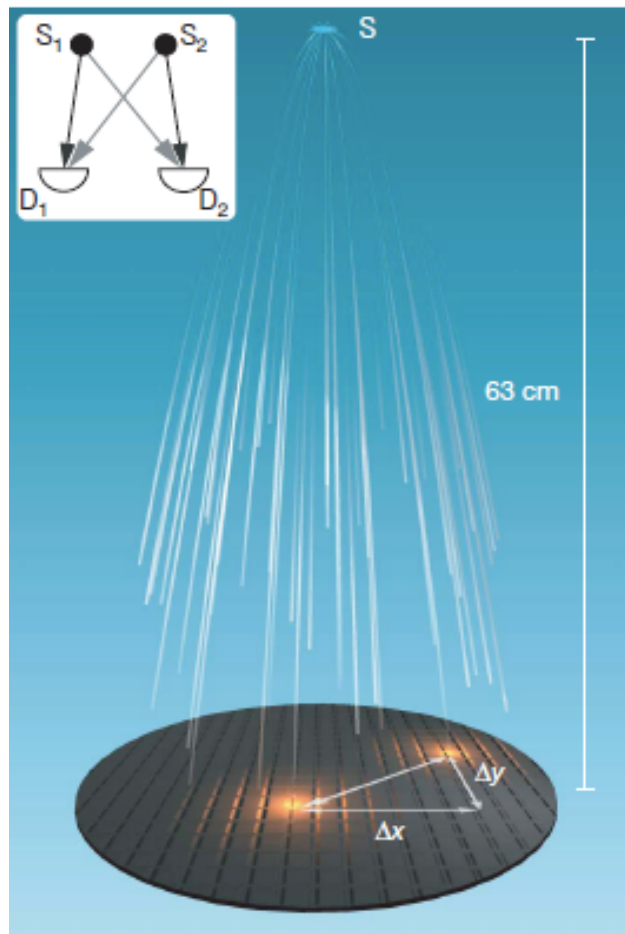
Detector resolution time $\sim 10^{-11}$ s

→ reduce effect by 1000

Unpolarized electrons → reduce effect by 2

Comparison of the Hanbury Brown–Twiss effect for bosons and fermions

T. Jelte¹, J. M. McNamara¹, W. Hogervorst¹, W. Vassen¹, V. Krachmalnicoff², M. Schellekens², A. Perrin², H. Chang², D. Boiron², A. Aspect² & C. I. Westbrook²



Indistinguishable bosons:

$$| \text{parallel lines} + \text{crossed lines} |^2$$

Indistinguishable fermions:

$$| \text{parallel lines} - \text{crossed lines} |^2$$

Question:

Why is the correlation length bigger for ^3He than for ^4He ?

Answer: $\ell \sim 1/m$

Distinguishable:

$$| \text{parallel lines} |^2 + | \text{crossed lines} |^2$$

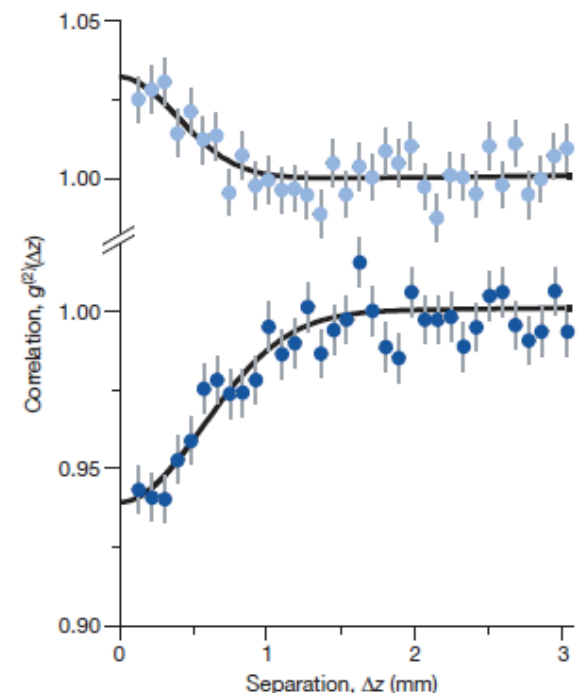


Figure 2 | Normalized correlation functions for $^4\text{He}^*$ (bosons) in the upper plot, and $^3\text{He}^*$ (fermions) in the lower plot. Both functions are measured at the same cloud temperature ($0.5\ \mu\text{K}$), and with identical trap parameters. Error bars correspond to the square root of the number of pairs in each bin.

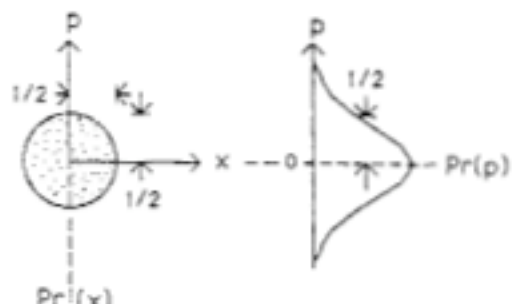
On $g^{(2)}$ of bosonic/fermionic atoms: “A value larger than 1 indicates bunching, while a value less than 1 is evidence of antibunching.”

-Jeltes et al. “Comparison of the Hanbury Brown-Twiss effect for bosons and fermions”, Nat. 2007

“Sub-Poisson counting statistics and anti-bunching are distinct effects, and it is important that the definitions of these phenomena not be confused.”

-Zou and Mandel, PRA 1990

Vacuum State



Coherent State

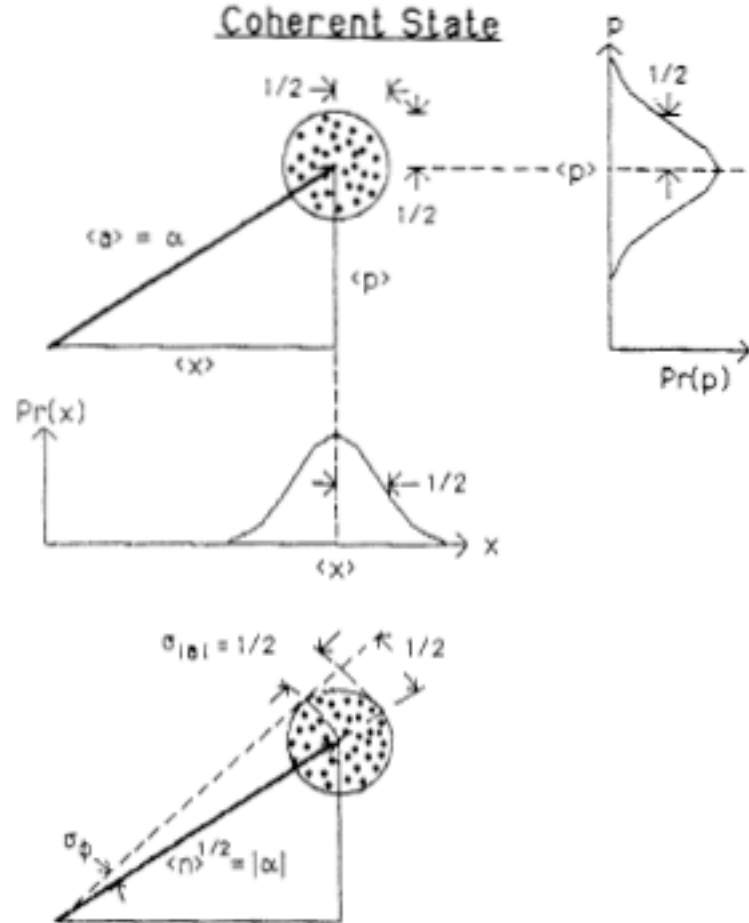


Figure 4. Quadrature-component and number-phase uncertainties for the coherent state.

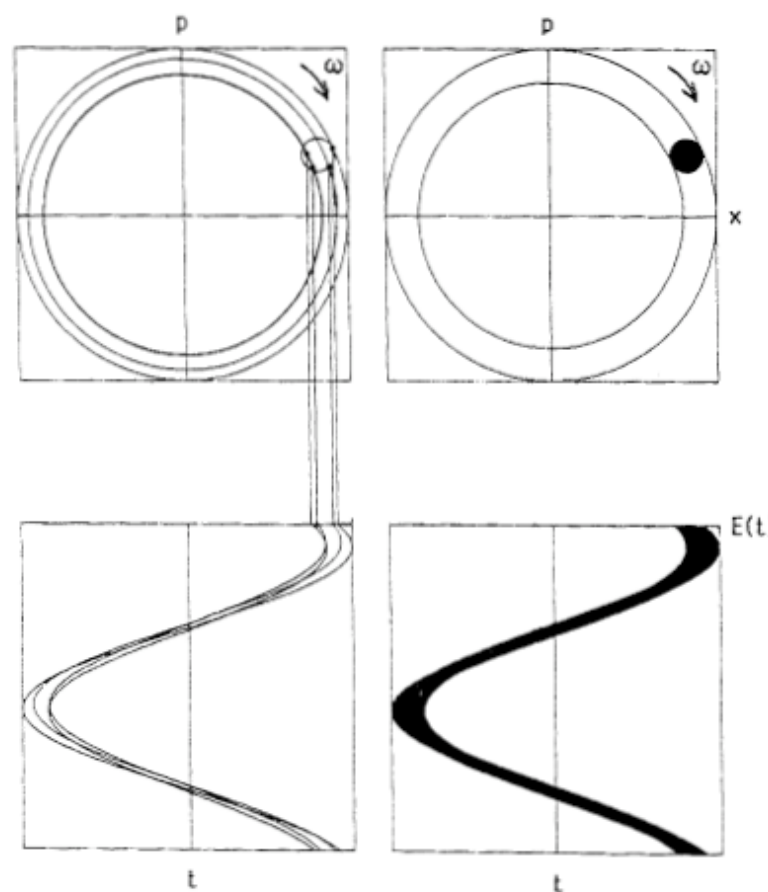
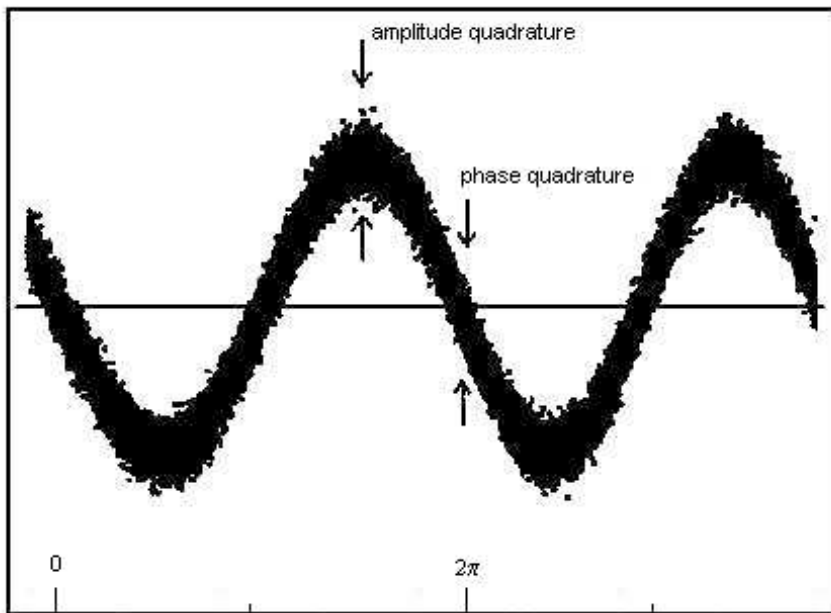
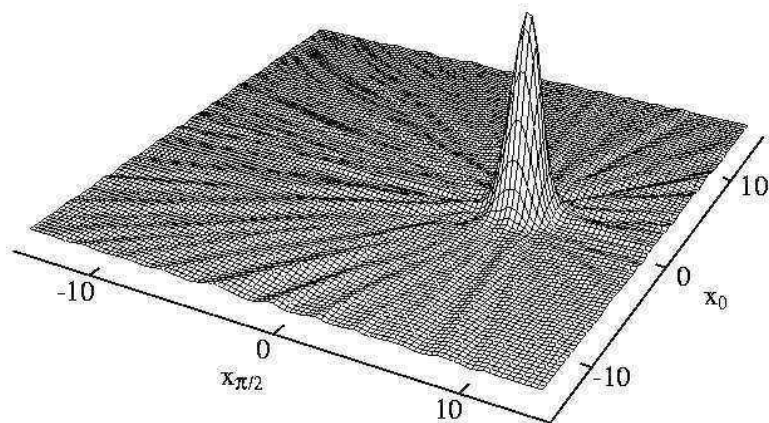


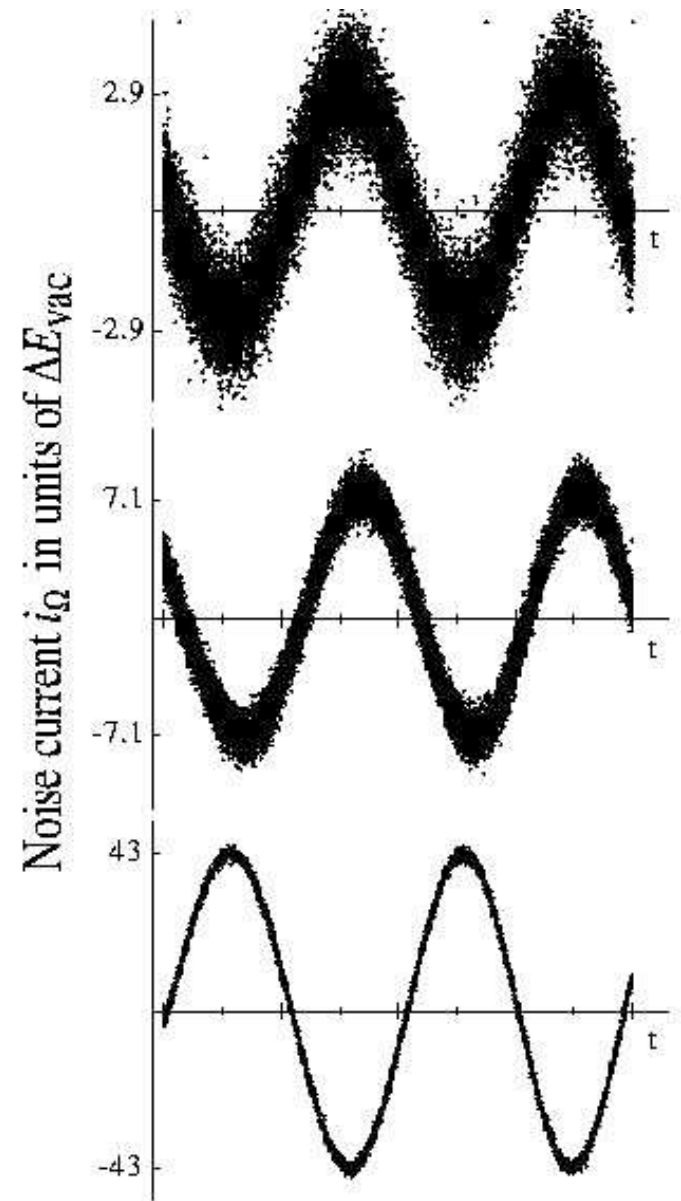
Figure 6. Electric-field time dependence for the coherent state.



Noise in coherent state does not depend on the phase.



Measured 'Wigner' distribution



Relative noise decreases as state amplitude increases.

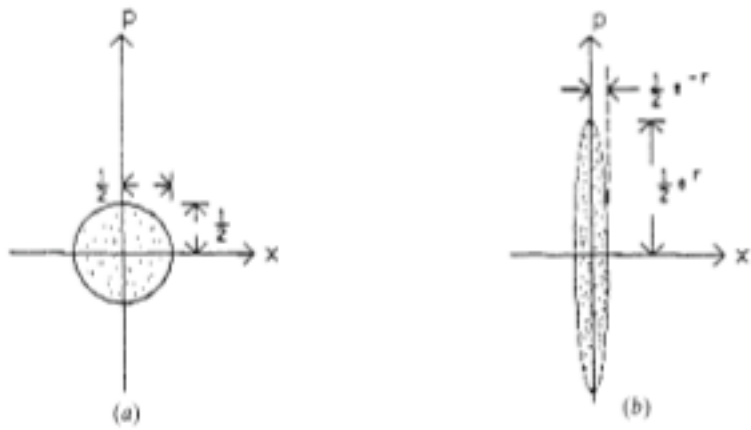


Figure 9. Comparison of quadrature-component uncertainties for the vacuum state: (a) vacuum state, (b) squeezed vacuum state.

Vacuum squeezed state

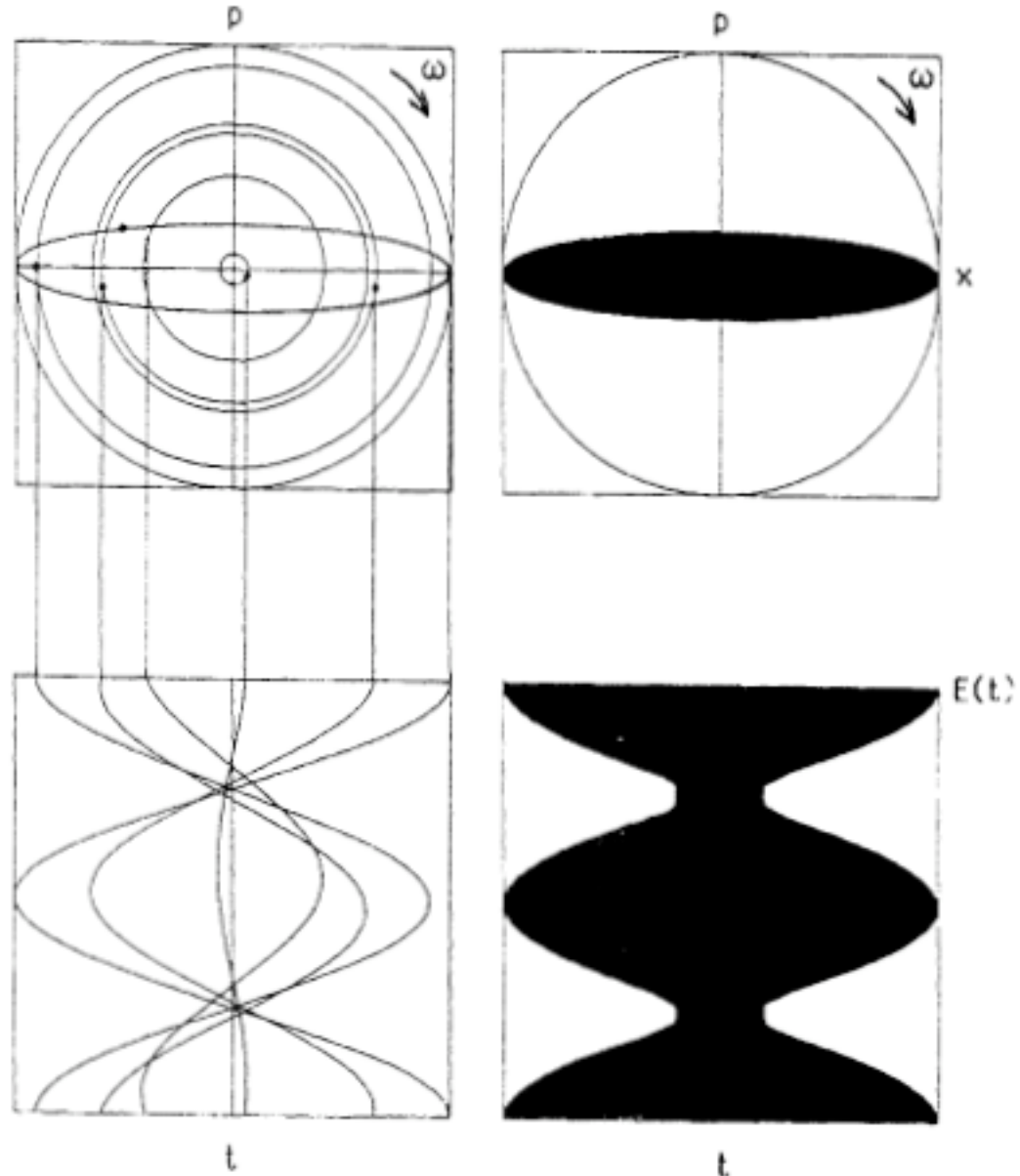
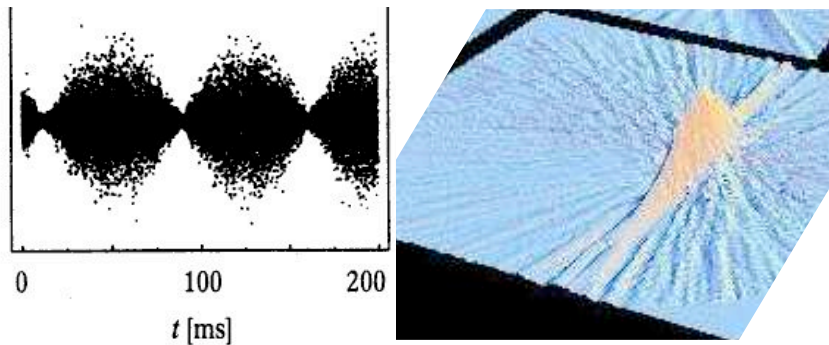
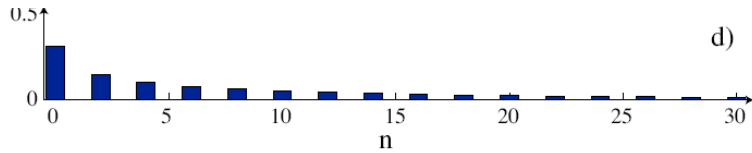


Figure 12. Electric-field time dependence for the squeezed vacuum state.

$g^{(2)}$ of a Squeezed Vacuum State

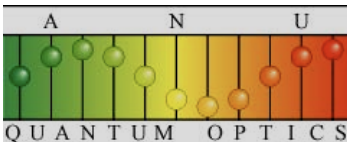
For a Vacuum squeezed state:

$$\begin{aligned}g^{(2)} &= \frac{\langle 0 | S^+(\xi) a^+ a^+ a a S(\xi) | 0 \rangle}{\langle 0 | S^+(\xi) a^+ a S(\xi) | 0 \rangle^2} \\ &= \frac{\langle 0 | S^+(\xi) a^+ S(\xi) S^+(\xi) a^+ S(\xi) S^+(\xi) a S(\xi) S^+(\xi) a S(\xi) | 0 \rangle}{\langle 0 | S^+(\xi) a^+ S(\xi) S^+(\xi) a S(\xi) | 0 \rangle^2}\end{aligned}$$

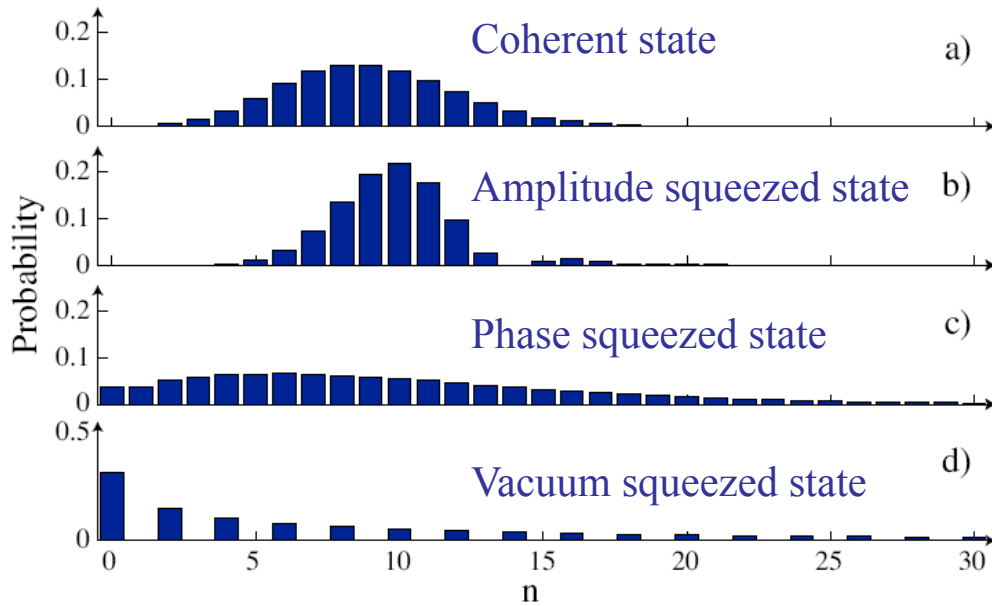
$$S^+(\xi) a S(\xi) = \cosh(\xi) a - e^{-2i\theta} \sinh(\xi) a^+$$

$$g^{(2)} = \frac{5 - 8 \cosh(2\xi) + 3 \cosh(4\xi)}{2(1 - \cosh(2\xi))^2}$$

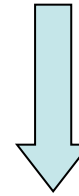
(see, for example, Walls and Milburn: Quantum Optics)



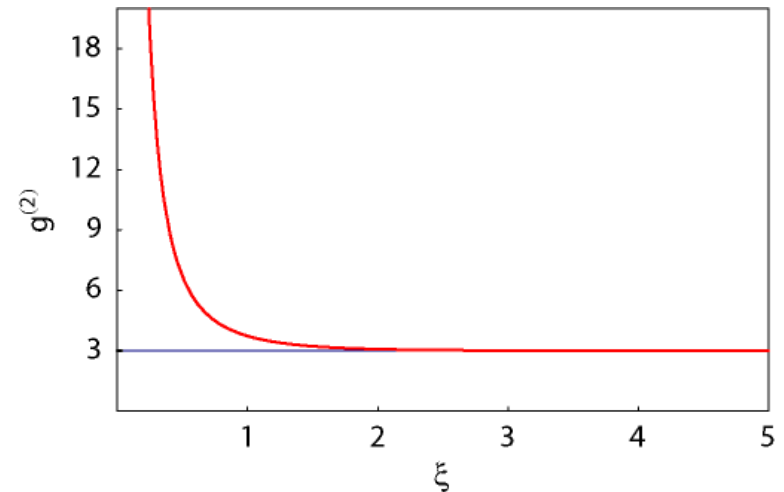
Photon Numbers for the SV State



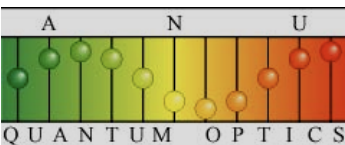
$$g^{(2)} = \frac{5 - 8 \cosh(2\xi) + 3 \cosh(4\xi)}{2(1 - \cosh(2\xi))^2}$$



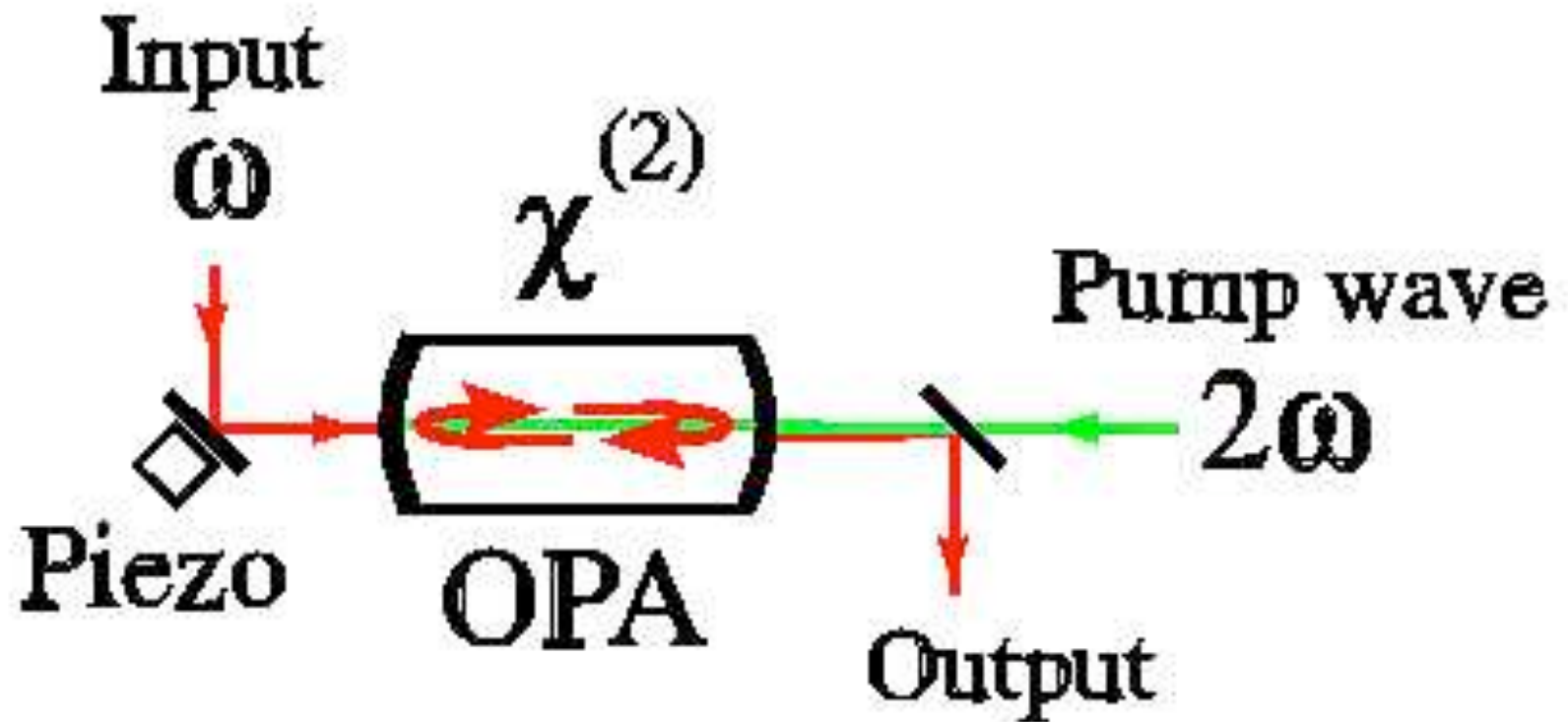
$$g^{(2)}(\xi \approx 0) \gg 3$$



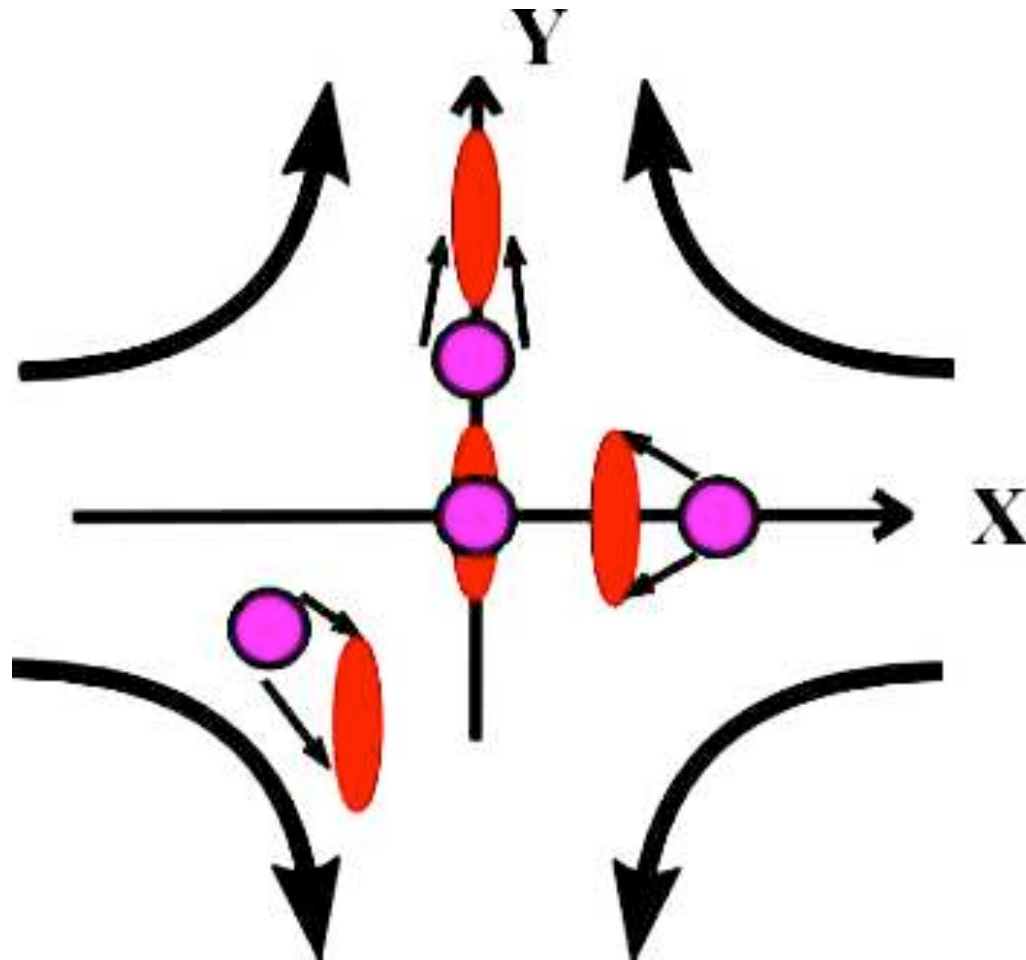
A vacuum squeezed state exhibits strong photon bunching



Phase-sensitive amplifier \rightarrow squeezing



Phase-sensitive amplifier \rightarrow squeezing



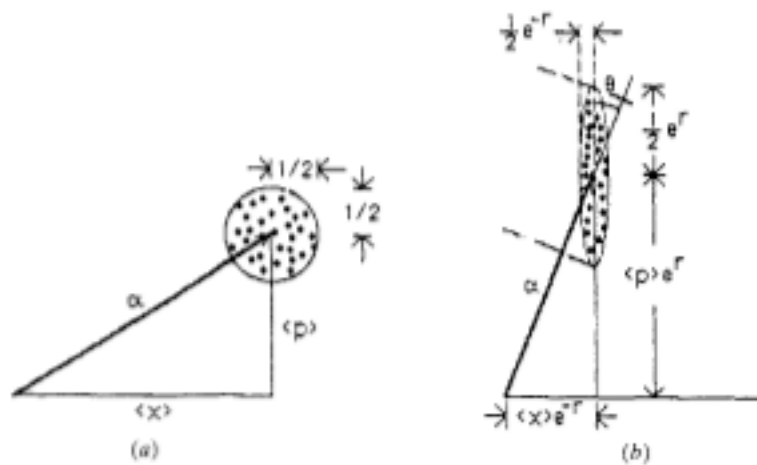


Figure 10. Comparison of quadrature-component uncertainties for the coherent and squeezed coherent states: (a) coherent state, (b) squeezed coherent state.

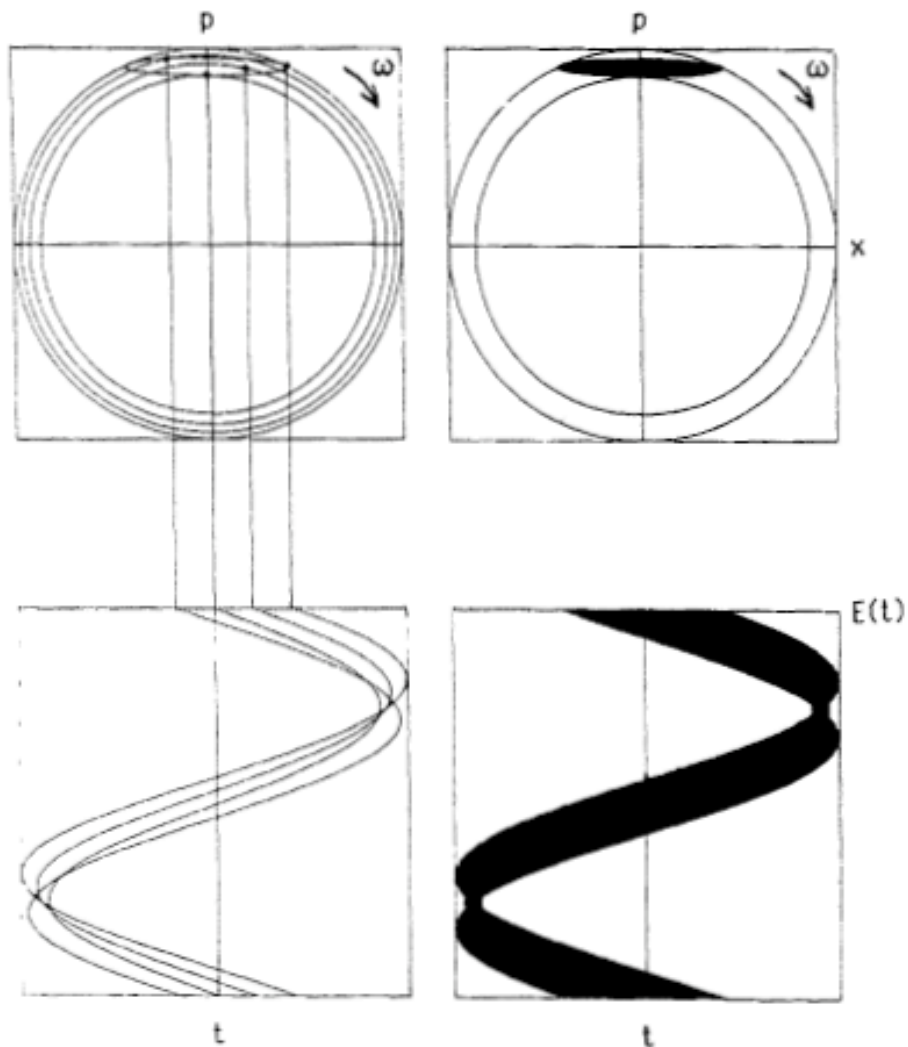


Figure 13. Electric-field time dependence for the squeezed coherent state.

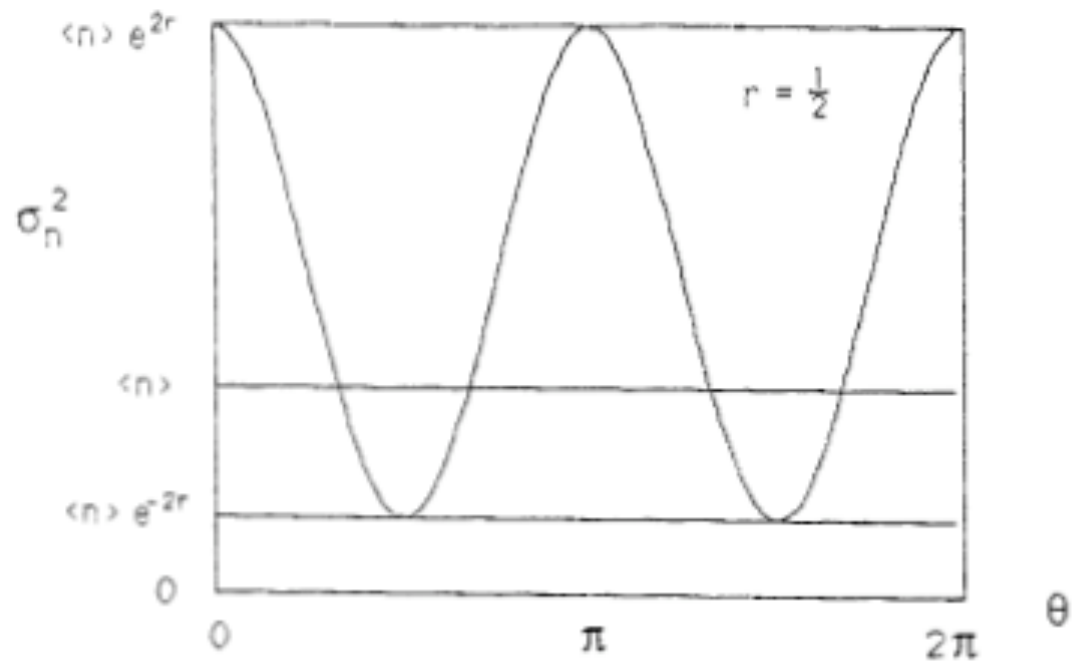
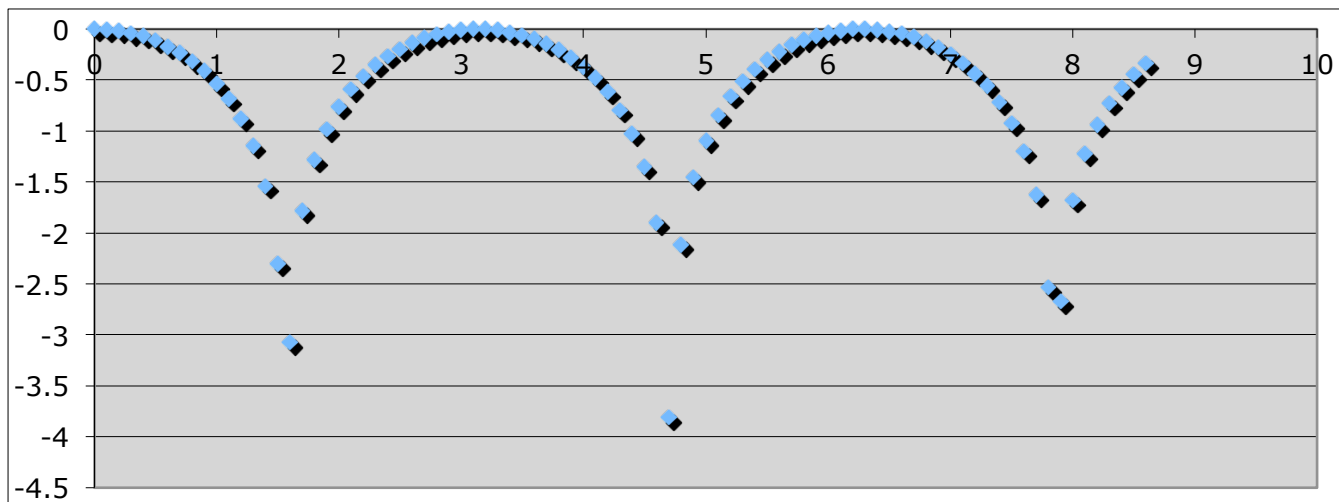


Figure 11. Dependence of the squeezed coherent state photon-number variance, σ_n^2 , on the angle θ . The light is super- or sub-Poisson depending on θ .



Measurement of the quantum states of squeezed light

G. Breitenbach, S. Schiller & J. Mlynek

Fakultät für Physik, Universität Konstanz, D-78457 Konstanz, Germany

NATURE | VOL 387 | 29 MAY 1997

A state of a quantum-mechanical system is completely described by a density matrix or a phase-space distribution such as the Wigner function. The complete family of squeezed states of light (states that have less uncertainty in one observable than does the vacuum state) have been generated using an optical parametric amplifier, and their density matrices and Wigner functions have been reconstructed from measurements of the quantum statistics of their electric fields.

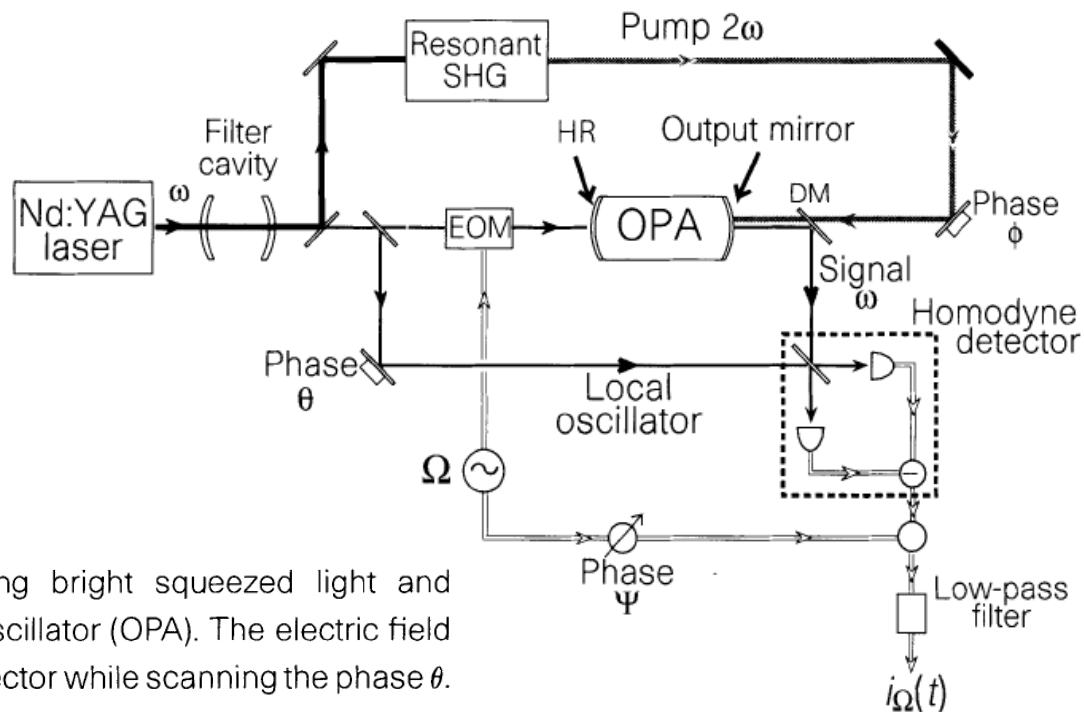


Figure 1 Experimental scheme for generating bright squeezed light and squeezed vacuum with an optical parametric oscillator (OPA). The electric field quadratures are measured in the homodyne detector while scanning the phase θ . A computer performs the statistical analysis of the photocurrent i_{Ω} and reconstructs the quantum states. EOM, electro-optic modulator; DM, dichroic mirror; SHG, second harmonic generator; HR, high reflector.

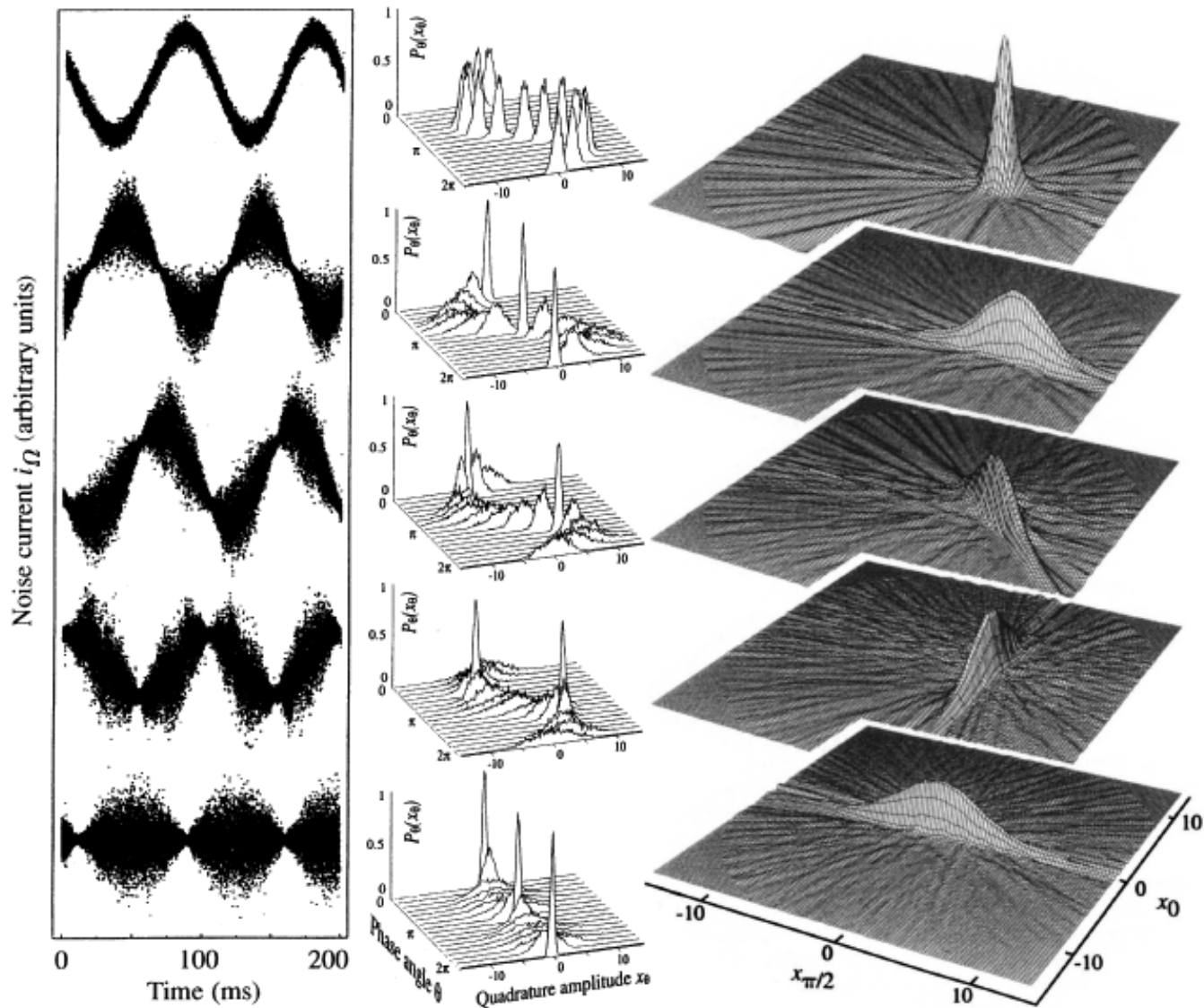


Figure 2 Noise traces in $i_Q(t)$ (left), quadrature distributions $P_\theta(x_0)$ (centre), and reconstructed Wigner functions (right) of generated quantum states. From the top: Coherent state, phase-squeezed state, state squeezed in the $\phi = 48^\circ$ -quadrature, amplitude-squeezed state, squeezed vacuum state. The noise traces as a function of time show the electric fields' oscillation in a 4π interval for the upper

four states, whereas for the squeezed vacuum (belonging to a different set of measurements) a 3π interval is shown. The quadrature distributions (centre) can be interpreted as the time evolution of wave packets (position probability densities) during one oscillation period. For the reconstruction of the quantum states a π interval suffices.

Observation of Squeezed Light with 10-dB Quantum-Noise Reduction

Benjamin Vahlbruch, Moritz Mehmet, Simon Chelkowski, Boris Hage, Alexander Franzen, Nico Lastzka, Stefan Gößler, Karsten Danzmann, and Roman Schnabel

Institut für Gravitationsphysik, Leibniz Universität Hannover and Max-Planck-Institut für Gravitationsphysik (Albert-Einstein-Institut), Callinstr. 38, 30167 Hannover, Germany

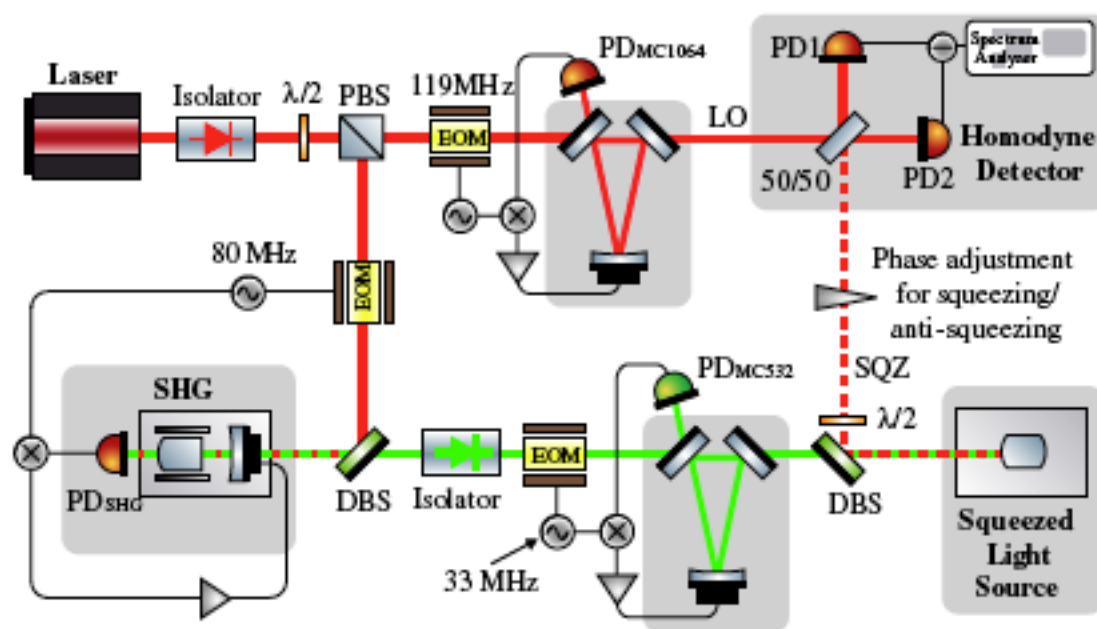


FIG. 1 (color online). Schematic of the experimental setup. Squeezed states of light (SQZ) at 1064 nm were generated by type I optical parametric oscillation (OPO) below threshold. SHG, Second harmonic generation (SHG); Polarizing beam splitter (PBS); Dichroic beam splitter (DBS); Local oscillator (LO), photodiode (PD); electro-optical modulator (EOM).

Same group: 12.7 dB squeezing \rightarrow noise reduced to $\sim 5\%$

PRL **104**, 251102 (2010)

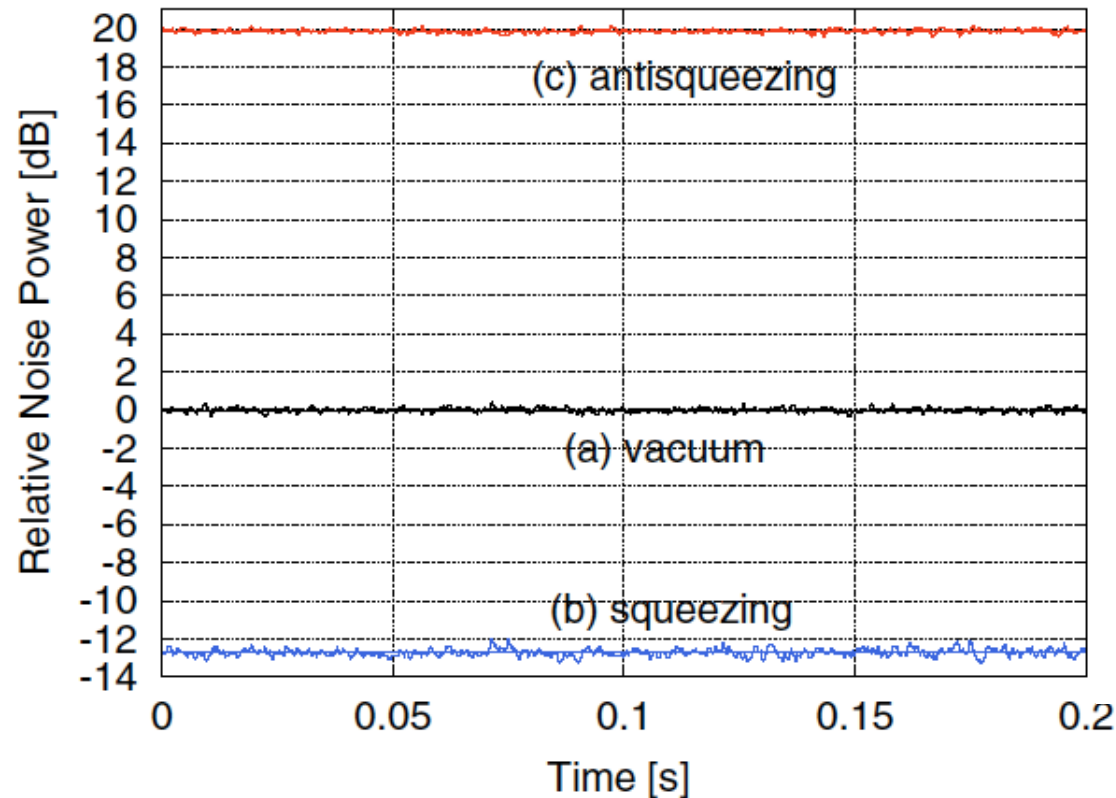


FIG. 3 (color online). Characterization of our squeezed-light laser at a sideband frequency of 5 MHz. All traces are normalized to the vacuum-noise reference of the homodyne detector's local oscillator beam (a). Trace (b) shows the noise in the squeezed field quadrature; trace (c) shows the antisqueezing in the orthogonal quadrature. Detector dark noise is at -25 dB and, here, *not* subtracted from the data.

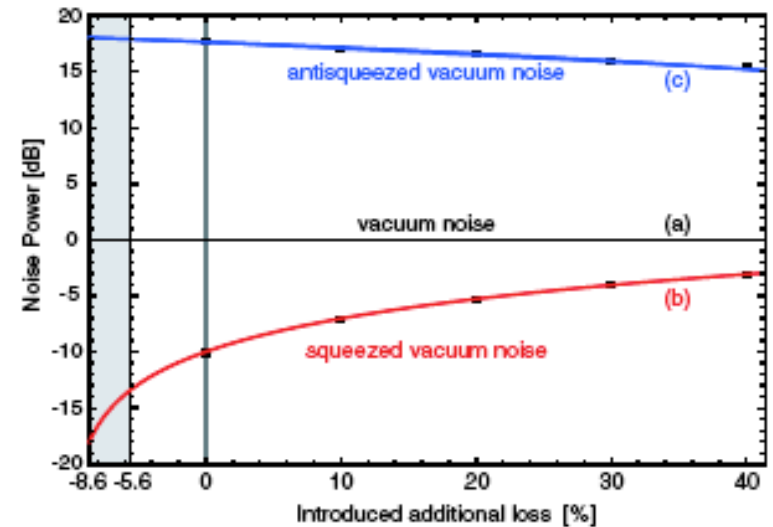


FIG. 4 (color online). Squeezing and antisqueezing levels for a parametric gain of 63 versus optical loss. Solid lines show the theoretical predictions. Square boxes represent measurement values with sizes corresponding to the errors bars. Electronic dark noise was subtracted in this figure. The two vertical axis on the left corresponds to the upper and lower boundaries of how much squeezing might be achieved in our setup by reduction of optical loss.

Loss reduces squeezing...

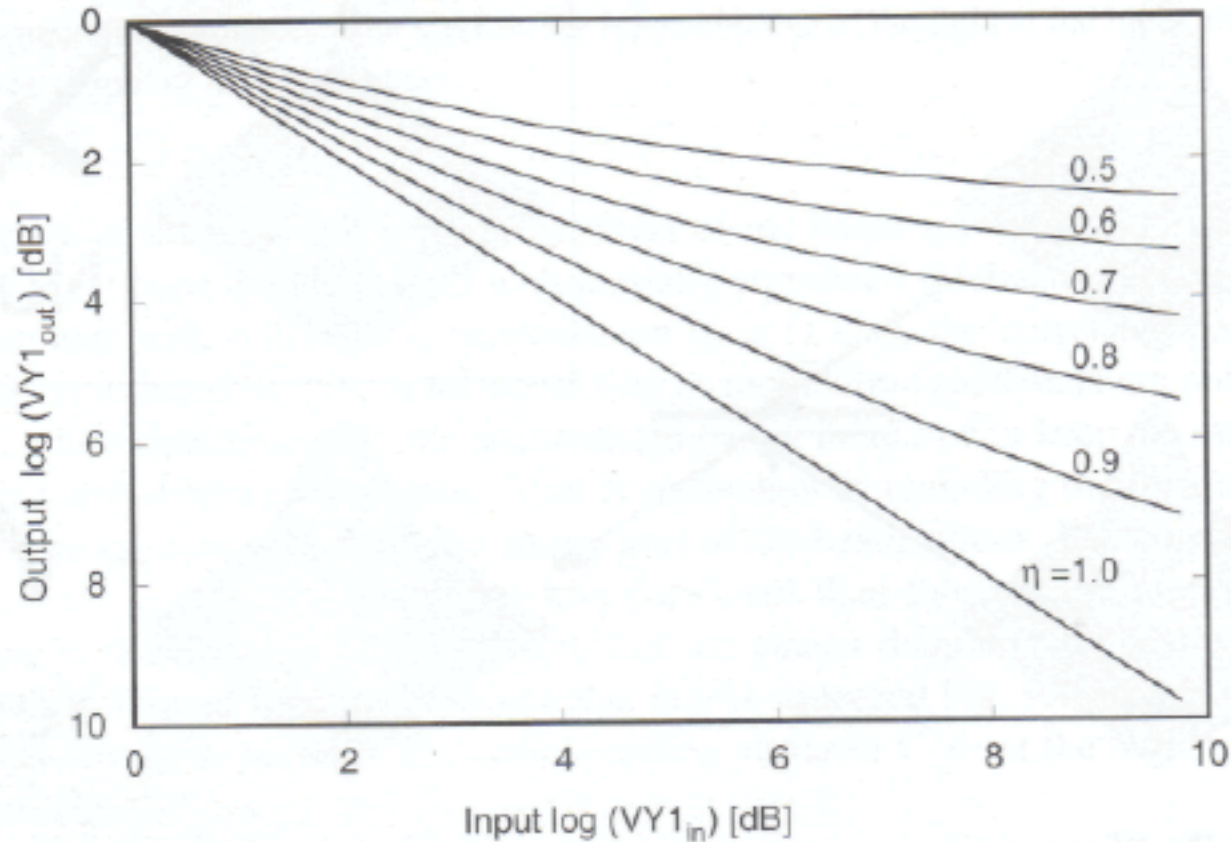


Figure 9.19: The quantitative effect of different efficiencies η on the minimum variance of the squeezed state.

A Quantum Laser Pointer

Nicolas Treps,^{1,2*} Nicolai Grosse,¹ Warwick P. Bowen,¹ Claude Fabre,² Hans-A. Bachor,¹ Ping Koy Lam¹

The measurement sensitivity of the pointing direction of a laser beam is ultimately limited by the quantum nature of light. To reduce this limit, we have experimentally produced a quantum laser pointer, a beam of light whose direction is measured with a precision greater than that possible for a usual laser beam. The laser pointer is generated by combining three different beams in three orthogonal transverse modes, two of them in a squeezed-vacuum state and one in an intense coherent field. The result provides a demonstration of multichannel spatial squeezing, along with its application to the improvement of beam positioning sensitivity and, more generally, to imaging.

15 AUGUST 2003 VOL 301 SCIENCE 940

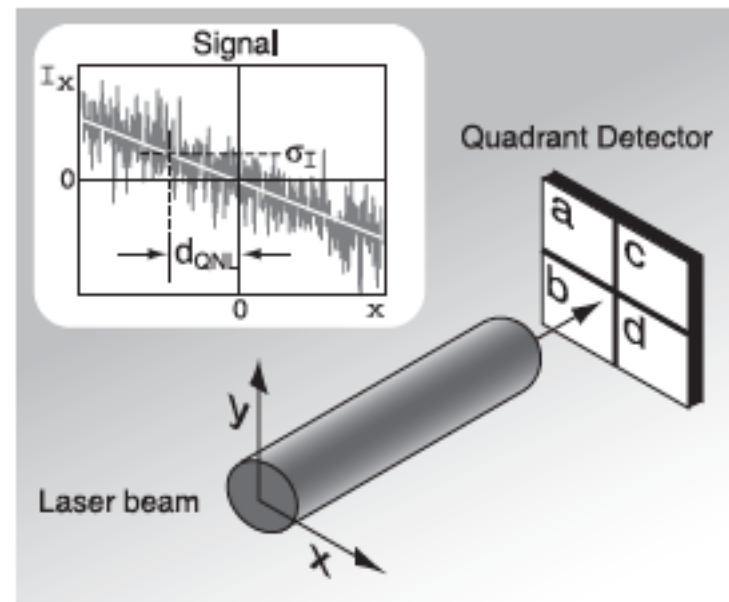
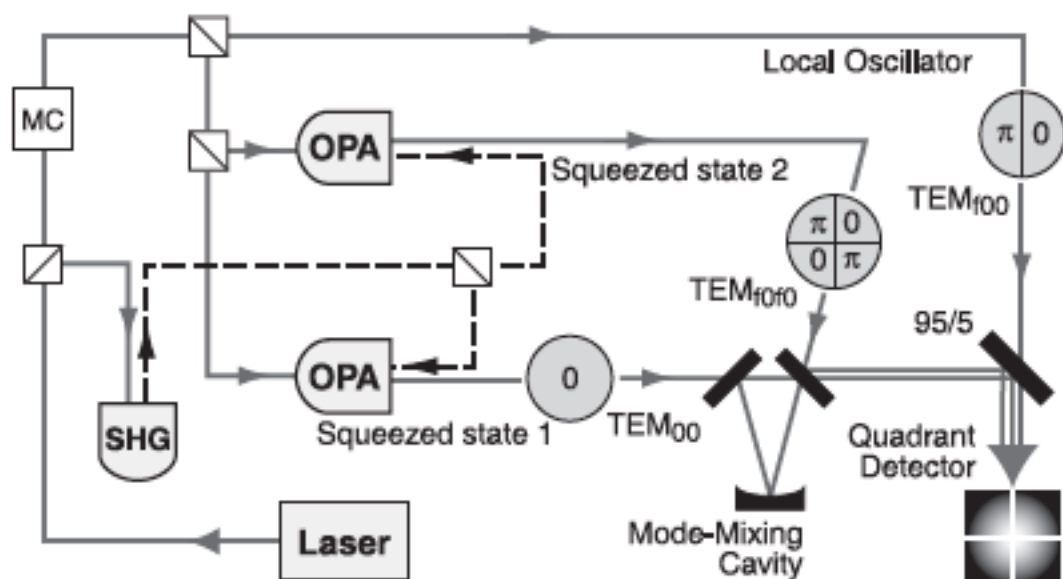
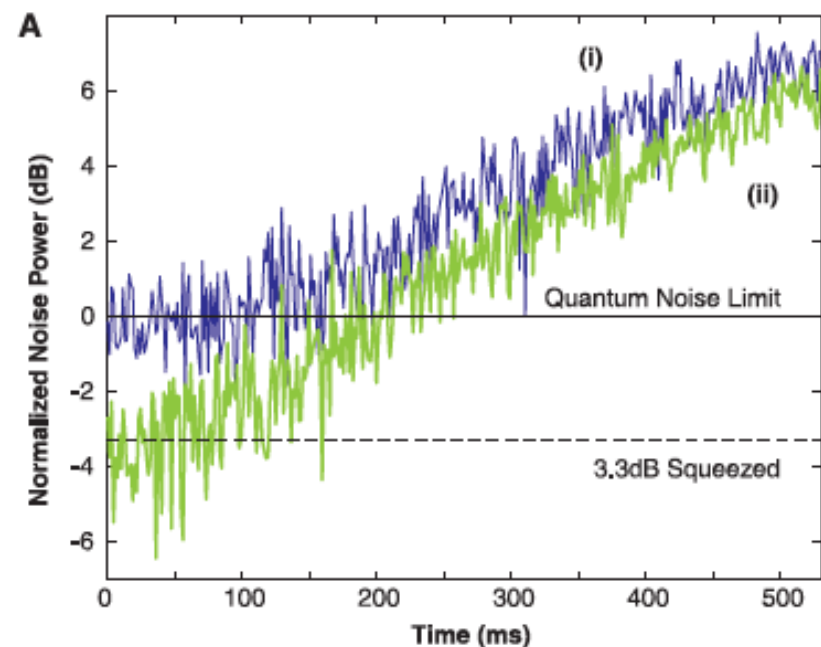
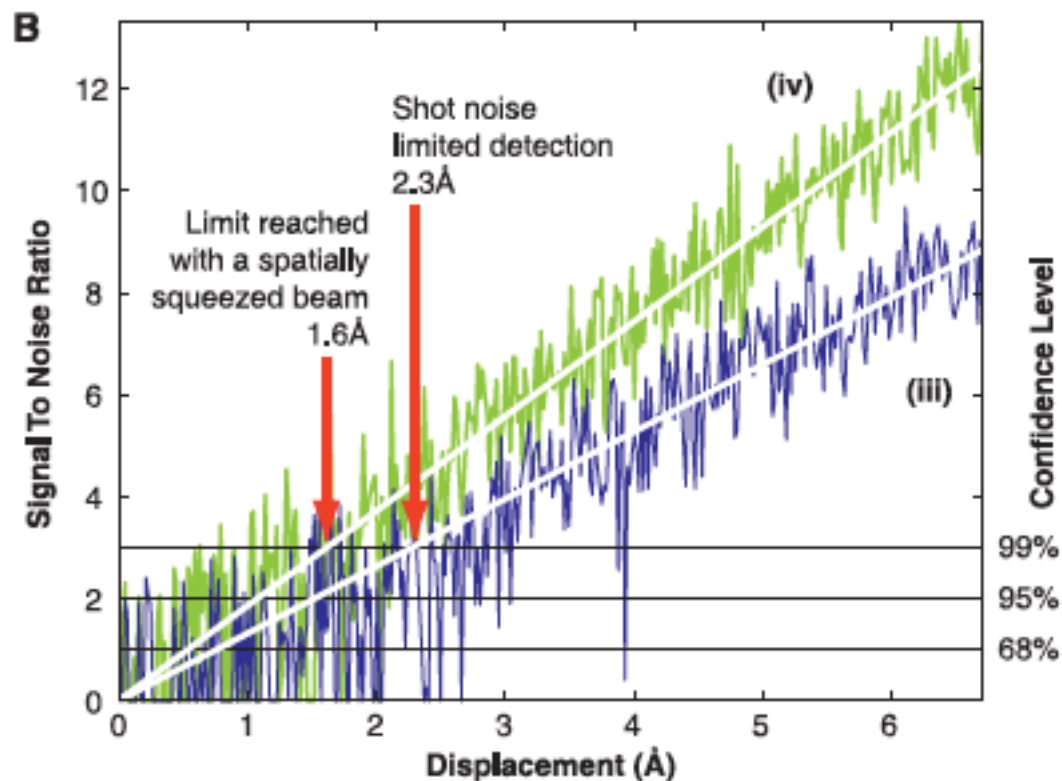


Fig. 1. Measurement of laser beam direction. A laser beam is incident on a quadrant detector. Simple arithmetic operations are performed on the four photo currents to produce signals I_x and I_y , which are proportional to the displacement in the horizontal and vertical axes, respectively. An example signal for I_x is plotted. The standard deviation of the signal σ_I defines the quantum noise limited displacement d_{QNL} .



Data from (A) processed to show signal-to-noise improvement (left vertical axis) plotted against the inferred displacement. Traces (iii) and (iv) show the results from data (i) and (ii), respectively. The squeezing translates into an increase in displacement sensitivity. Choosing a 99% confidence level (right vertical axis), the smallest displacement detectable improved from 2.3 to 1.6 Å.

Fig. 2. (A) Measurement of horizontal displacement signal ramped up in time, with (i) coherent beams and (ii) spatially squeezed beams. Both radio-frequency spectrum analyzer traces are the averages of 20 runs with $VBW = RBW = 1$ kHz. The observed noise reduction of the squeezed beams measurement is 3.3 ± 0.2 dB. **(B)**



Newest Application of Squeezing...

PHYSICAL REVIEW X 4, 011017 (2014)

Subdiffraction-Limited Quantum Imaging within a Living Cell

Michael A. Taylor,^{1,2} Jiri Janousek,³ Vincent Daria,⁴ Joachim Knittel,¹ Boris Hage,^{3,5}
Hans-A. Bachor,^{3,4} and Warwick P. Bowen^{2*}

¹*Department of Physics, University of Queensland, St Lucia, Queensland 4072, Australia*

²*Centre for Engineered Quantum Systems, University of Queensland,
St Lucia, Queensland 4072, Australia*

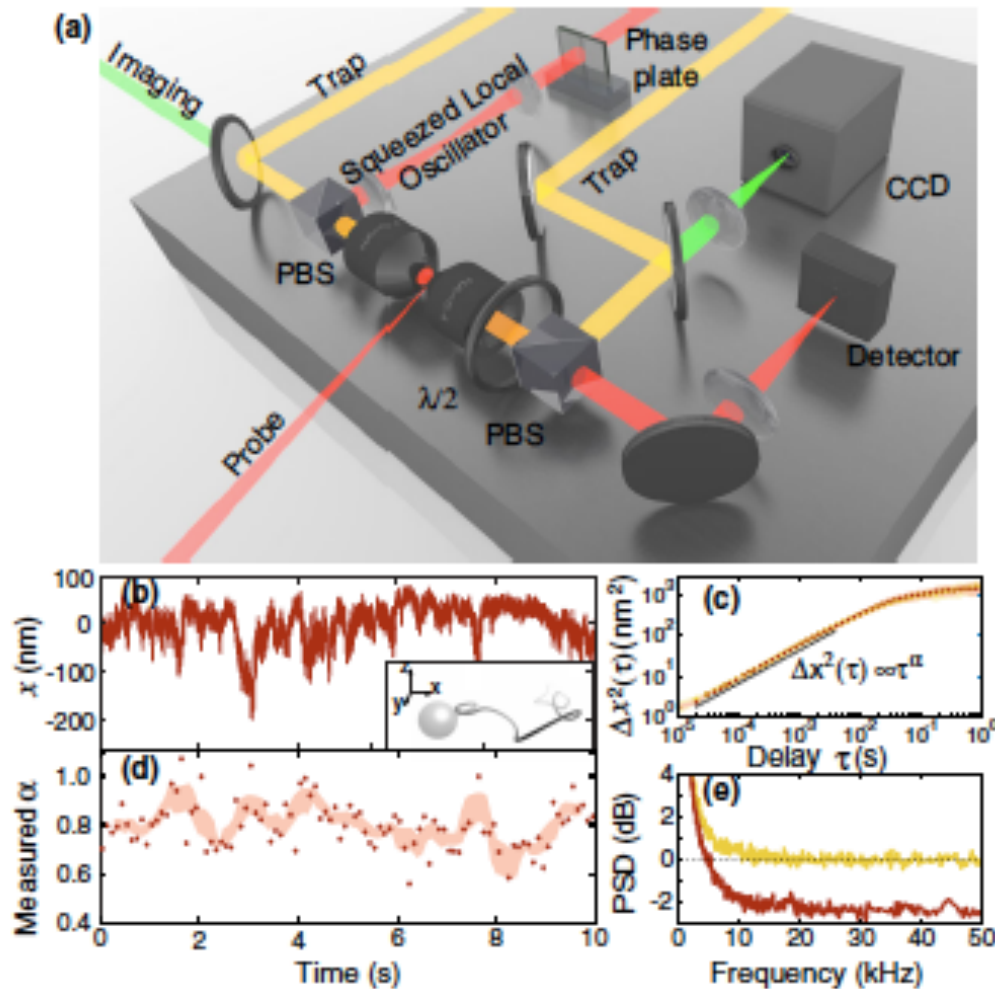
³*Department of Quantum Science, Australian National University, Canberra,
Australian Capital Territory 0200, Australia*

⁴*John Curtin School of Medical Research, Australian National University, Canberra,
Australian Capital Territory 0200, Australia*

⁵*Institut für Physik, Universität Rostock, D-18051 Rostock, Germany*

(Received 21 October 2013; revised manuscript received 16 December 2013; published 4 February 2014)

We report both subdiffraction-limited quantum metrology and quantum-enhanced spatial resolution for the first time in a biological context. Nanoparticles are tracked with quantum-correlated light as they diffuse through an extended region of a living cell in a quantum-enhanced photonic-force microscope. This allows spatial structure within the cell to be mapped at length scales down to 10 nm. Control experiments in water show a 14% resolution enhancement compared to experiments with coherent light. Our results confirm the long-standing prediction that quantum-correlated light can enhance spatial resolution at the nanoscale and in biology. Combined with state-of-the-art quantum light sources, this technique provides a path towards an order of magnitude improvement in resolution over similar classical imaging techniques.



Saw structure on 10-nm scale,
with 14% better resolution than
using coherent light.

mechanical properties of the cytoplasm directly surrounding the nanoparticle could be characterized from its mean-squared displacement (MSD) after a delay τ ,

$$\langle \Delta x^2(\tau) \rangle = \langle (x(t) - x(t - \tau))^2 \rangle, \quad (1)$$

with an example shown in Fig. 1(c). Squeezed light improves the precision by reducing the error with which the MSD can be estimated. This improvement is shown in the measured power spectral density [Fig. 1(e)], with squeezed light lowering the noise floor by 2.4 dB. For short delays, the MSD is dominated by thermal motion and has the form

$$\langle \Delta x^2(\tau) \rangle = 2D\tau^\alpha, \quad (2)$$

$\alpha = 1$: diffusive

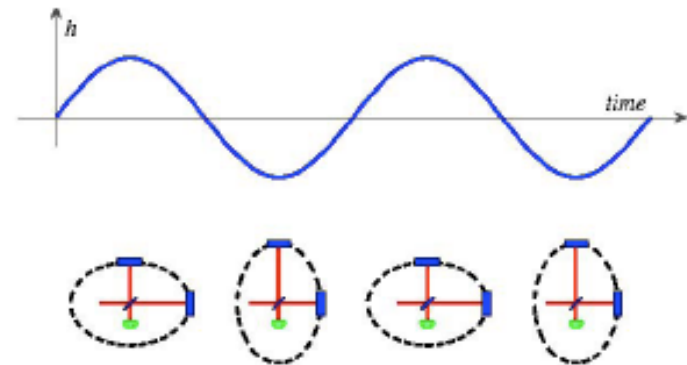
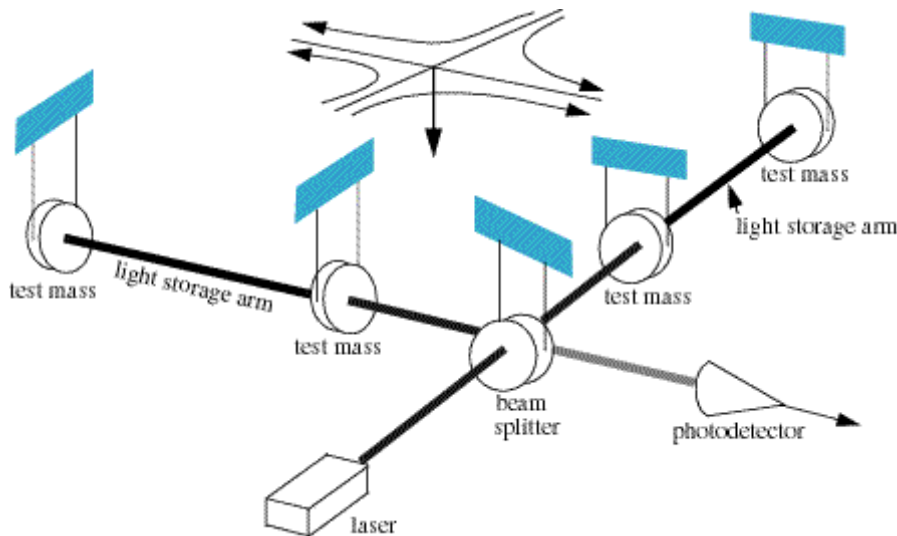
$\alpha < 1$: sub-diffusive-- particle confined;
cytoplasm has viscosity & elasticity

$\alpha > 1$: ballistic

FIG. 1 (color online). Experimental setup. (a) Counterpropagating trapping fields (orange) confine particles between two objectives and are isolated from the detector with polarizing beam splitters (PBS) and wave plates ($\lambda/2$). An imaging field (green) allows visual identification of the particles near the optical trap on a CCD camera. The particle tracking measurement relies only on an amplitude-squeezed local oscillator and an amplitude-modulated probe (red), with the probe providing dark-field illumination, and the particle tracking signal arising from interference between scattered light from the probe and the local oscillator. (b) Measured particle motion, which is the x projection of the 3D motion (shown schematically in the inset). (c) The MSD is constructed with both squeezed light (dark red) and coherent light (gold), and α is determined by fitting this to Eq. (2). The classical and squeezed example traces here both yield $\alpha = 0.83$. (d) The raw data are divided into 100 ms segments and the value of α established for each (solid dots). The light red shaded region represents the moving mean and standard error with a 0.5-s width. (e) The normalized power spectral density (PSD) shows that squeezing suppresses the noise floor by 2.4 dB.

Application: Gravity Wave Detection

- Einstein predicted that when massive objects accelerate, they produce time-dependent gravitational fields - gravity waves - that propagate as “warpings” of spacetime at the speed of light. (\sim EM radiation from accelerating e)
- The effect is very tiny: E.g., estimated $\Delta L/L$ of $\sim 10^{-21}$ for in-spiraling binary neutron stars. How to detect this???



The LIGO Collaboration, Rep.
Prog. Phys. 72, 076901 (2009).

Michelson operated on a dark fringe \rightarrow (ideally) only optical signals induced by asymmetric motion of arm-cavity mirrors exit the dark port of the beam splitter.

Application: Gravity Wave Detection

LIGO:

Laser

Interferometric

Gravitational wave

Observatory



-World's largest interferometers: 4-km

-2 in Hanford, WA; 1 in Livingston, LO

- >500 scientists

-Achieved sensitivity $\Delta L/L \sim 3 \times 10^{-23} \rightarrow \Delta L \sim 10^{-20} \text{ m}$

-Six data runs completed

-"Advanced LIGO" should improve sensitivity by another 10x

Scientists may have just discovered Einstein's gravitational waves

Published time: 12 Jan, 2016 13:46

[Get short URL](#)



“

My earlier rumor about LIGO has been confirmed by independent sources. Stay tuned! Gravitational waves may have been discovered!! Exciting.

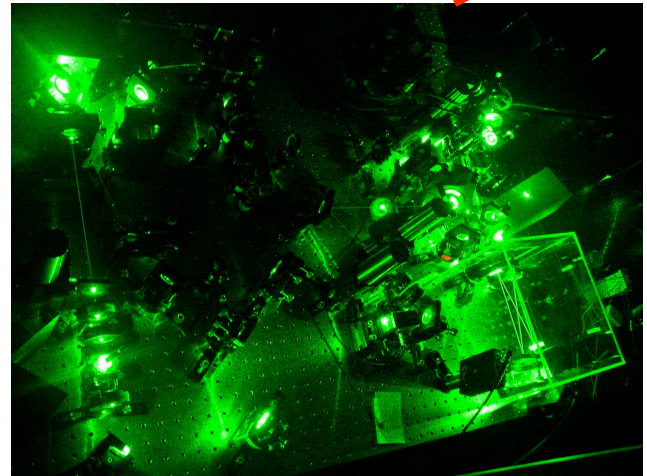
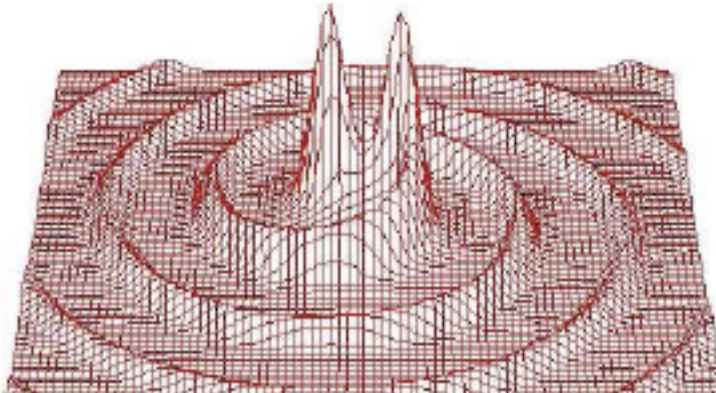
— Lawrence M. Krauss (@LKrauss1) [January 11, 2016](#)

”

LIGO – or Laser Interferometer Gravitational Wave Observatory – is one of several active experiments aimed at detecting the elusive ripples. It's recently gained an upgrade, dubbed Advanced LIGO. Completed last year, it is our latest and most promising stab at detection.

But LIGO, as well as Krauss, also found cause for jubilation last year, after the launch of the new souped-up version. However, at the time Krauss only gave it a 10-15 percent chance, while the LIGO team had said it was still analyzing data, which was *“the official response”* [cited](#) by the journal Nature.

Squeezing for Gravitational Wave Detection



- 1981 C.M. Caves (PRD 23:1693)
 - Squeezed states properly injected into an interferometer to circumvent SQL at high frequency where photon noise dominates

Two Types of Quantum Noise

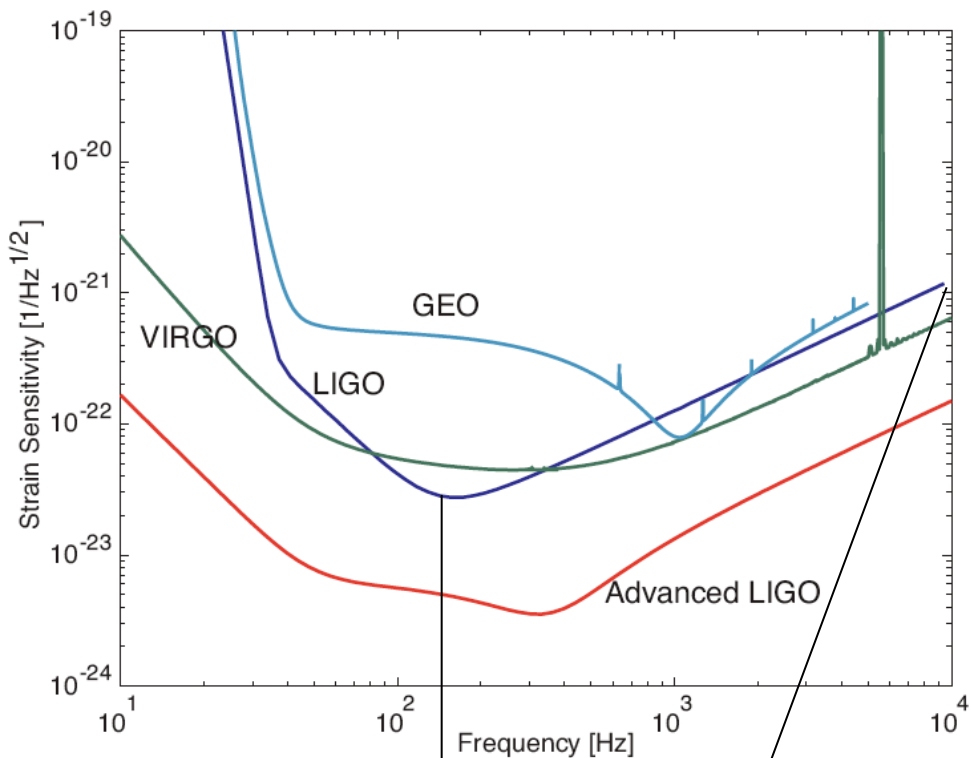
Shot noise: fluctuations in the number of photons leaving the interferometer. These can be seen as arising from phase noise entering via the (unused) vacuum port of the interferometer. As the input laser power increases, this phase uncertainty decreases \rightarrow use more power.

Radiation pressure noise: fluctuations in the differences of the locations of the end mirrors, due to fluctuations in the radiation pressure exerted by the light on the mirrors, in turn due to random scattering of the input photons at the beamsplitter. This noise increases with laser power.

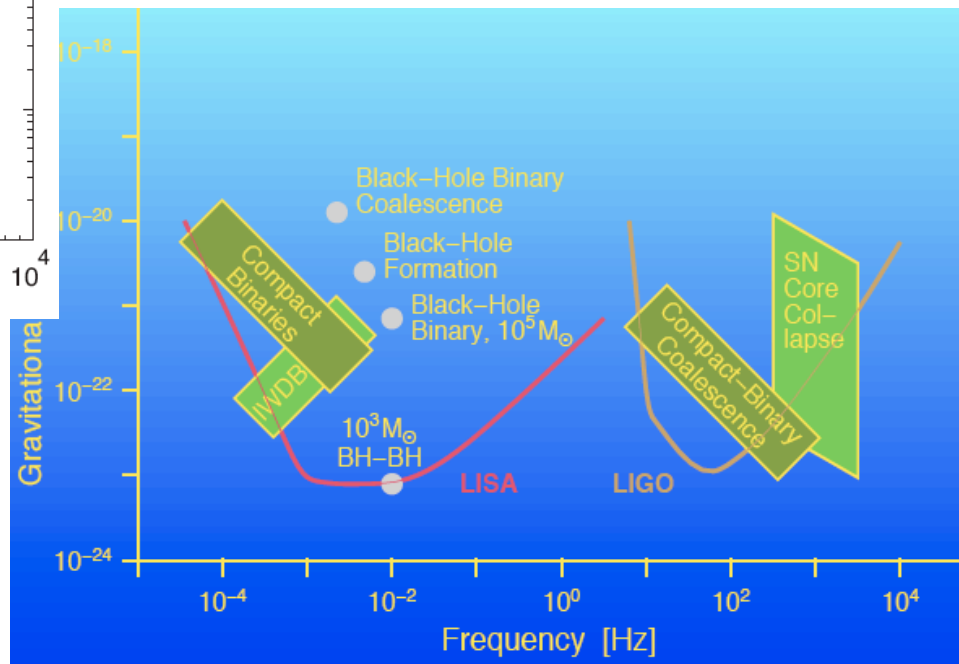
Standard Quantum Limit is reached at a power equalizing these: not attainable with current available laser powers \rightarrow interferometer is shot-noise limited ($\Delta z \sim \Delta \Phi \sim 1/\sqrt{N}$)

Caves: Used quadrature-squeezed input to reduce fluctuations.

Gravitational Wave - Quantum Noise Limited Window

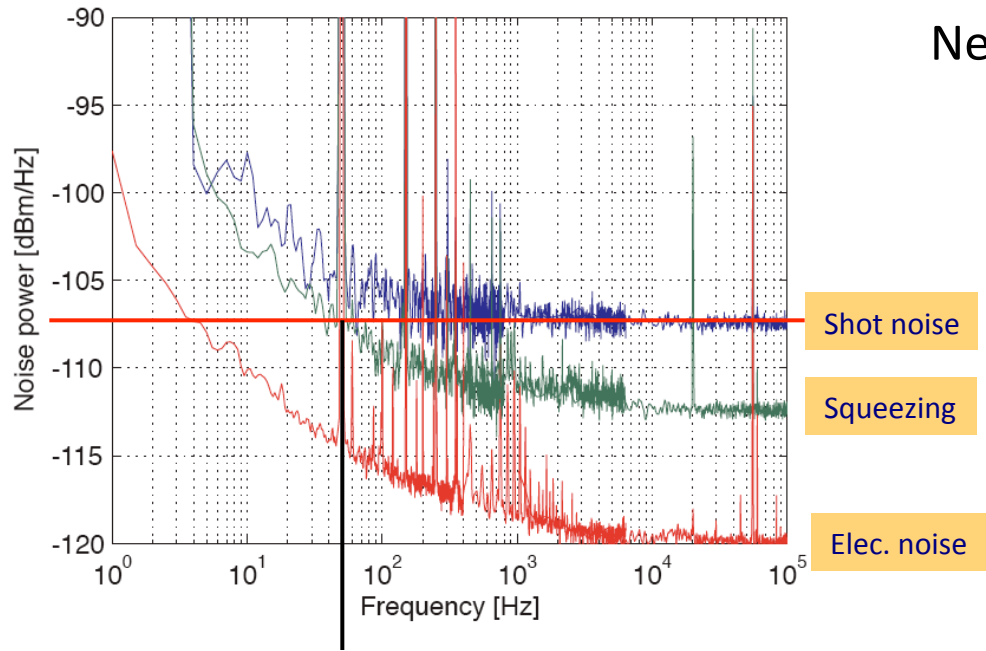


Gravitational Wave @ 10Hz-10kHz:



Quantum Noise Limited Regime

Audio Frequency Squeezing



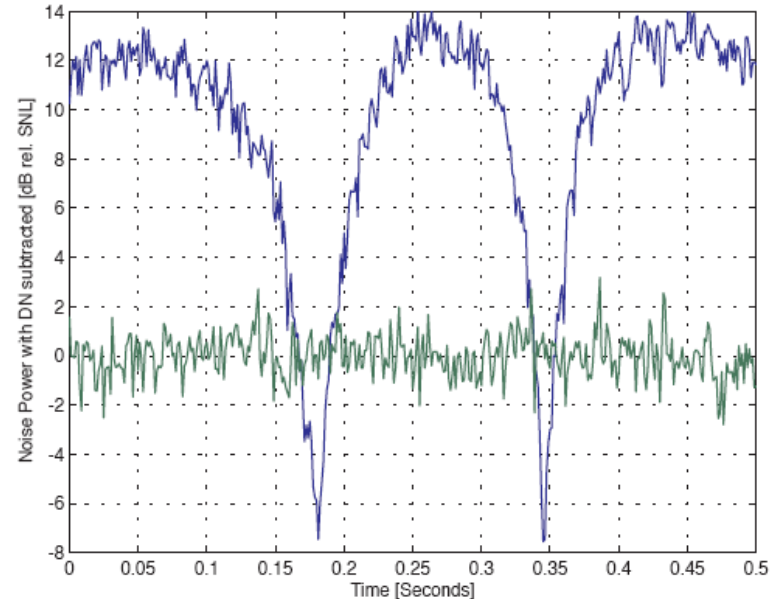
New Techniques

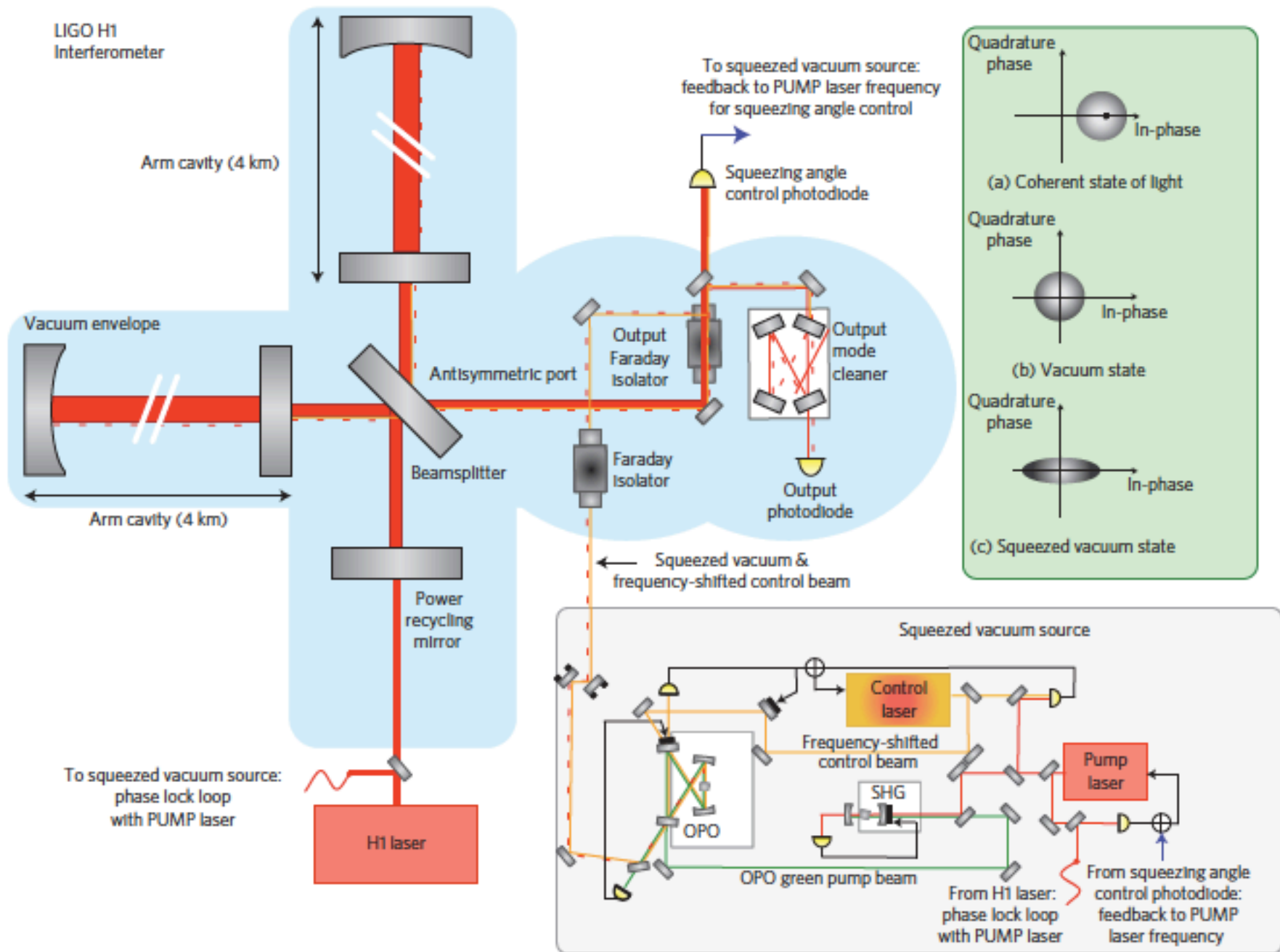
- Optical phase matching locking with effective temperature stability of ~ 10 's microK
- Quantum noise locking instead of PDH locking on the squeezed vacuum
- PPKTP doubly resonant OPO
- Eliminations of thermal, laser, dust, photo-thermal, mount, beam pointing, and seismic noises.

Squeezing Results

- >6 dB squeezing @ around 100 kHz
- Limited by escape eff., detector eff. and photo-thermal effect.
- Directly observed squeezing @ ~ 40 Hz
- Can see squeezing @ < 10 Hz

Currently Collaborating with LIGO on a 40m Michelson Interferometer





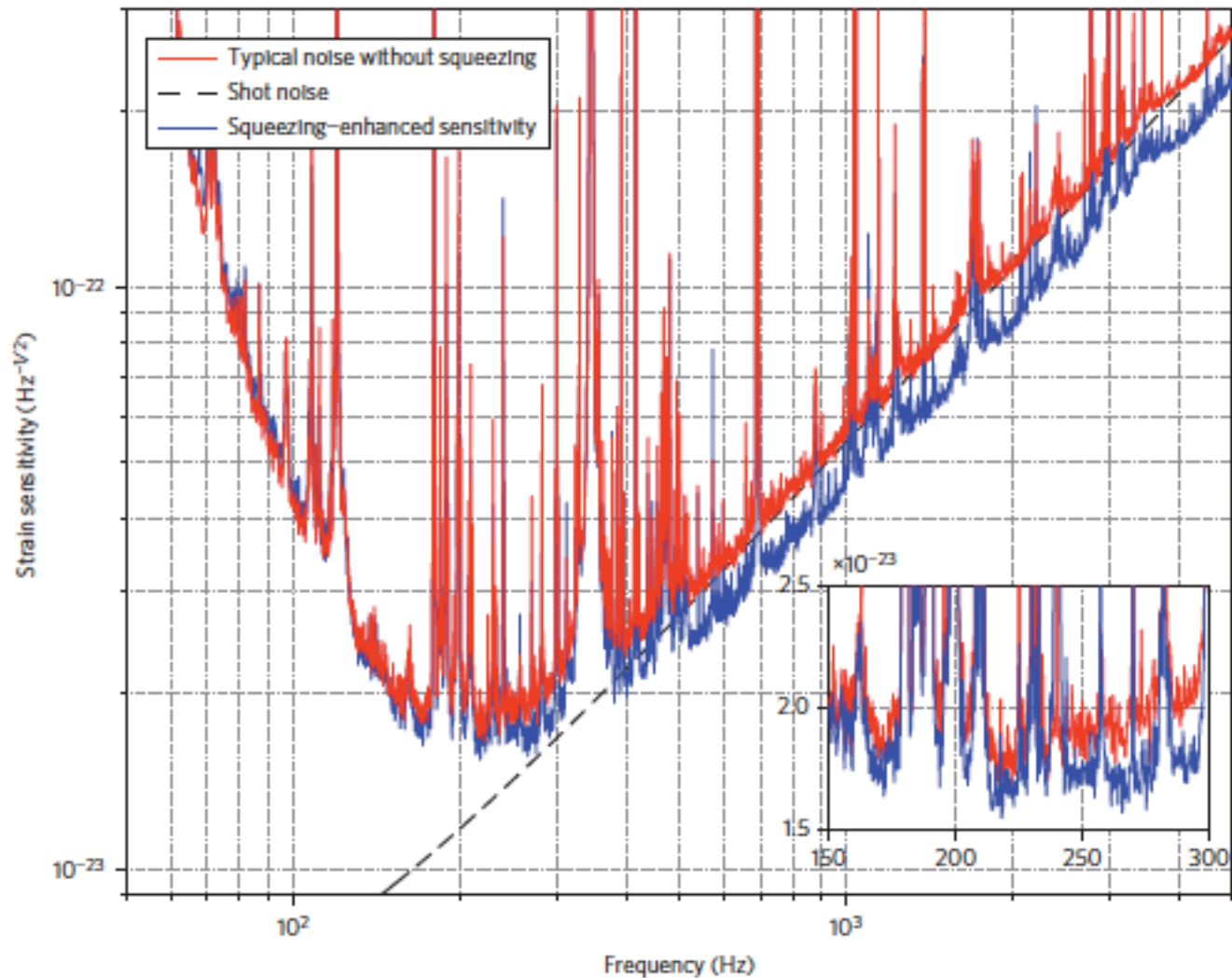


Figure 2 | Strain sensitivity of the H1 detector measured with and without squeezing injection. The improvement is up to 2.15 dB in the shot-noise-limited frequency band. Several effects cause the sharp lines visible in the spectra: mechanical resonances in the mirror suspensions, resonances of the internal mirror modes, power line harmonics and so on. As the broadband floor of the sensitivity is most relevant for gravitational-wave detection, these lines are typically not too harmful. The inset magnifies the frequency region between 150 and 300 Hz, showing that the squeezing enhancement persists down to 150 Hz.

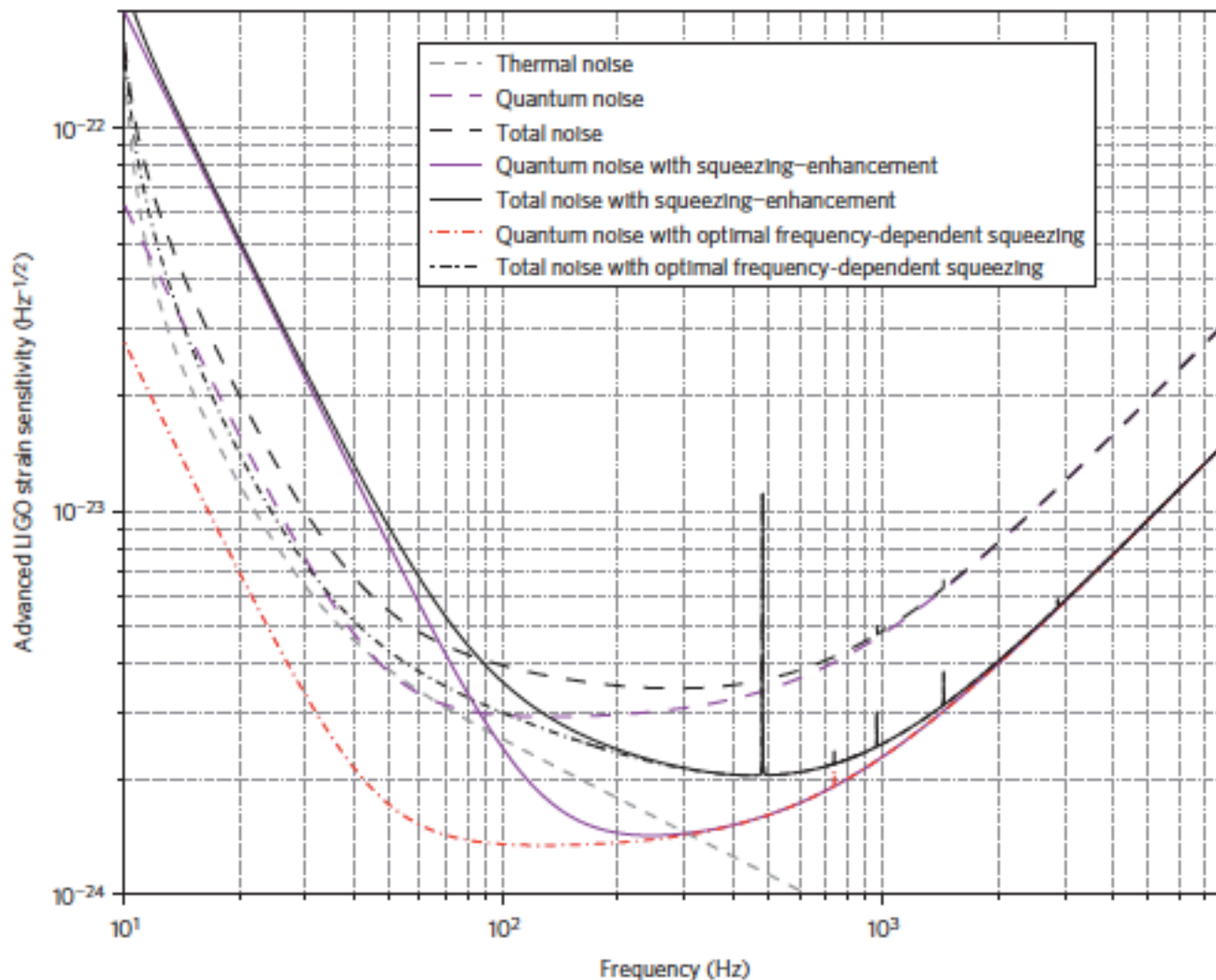


Figure 3 | Comparison of possible sensitivity curves for Advanced LIGO. Projection for a squeezing-enhanced Advanced LIGO interferometer (continuous lines), using a design similar to the one described in this Letter, is compared to the Advanced LIGO sensitivity tuned for high-frequency performance (dashed lines). The total noise, in both cases, has been computed by considering all the main noise sources, but only thermal noise and quantum noise are shown, as they are the only relevant noise sources above 100 Hz. The total losses for the squeezed beam were assumed to be 10%, starting with 9 dB of squeezing delivered by the OPO and 35 mrad of phase noise. With the same parameters, but assuming the injection of optimal frequency-dependent squeezing, quantum noise can be reduced at all frequencies, as shown by the dash-dotted red line.

Observation of Radiation Pressure Shot Noise on a Macroscopic Object

T. P. Purdy,^{1,2*} R. W. Peterson,^{1,2} C. A. Regal^{1,2}

The quantum mechanics of position measurement of a macroscopic object is typically inaccessible because of strong coupling to the environment and classical noise. In this work, we monitor a mechanical resonator subject to an increasingly strong continuous position measurement and observe a quantum mechanical back-action force that rises in accordance with the Heisenberg uncertainty limit. For our optically based position measurements, the back-action takes the form of a fluctuating radiation pressure from the Poisson-distributed photons in the coherent measurement field, termed radiation pressure shot noise. We demonstrate a back-action force that is comparable in magnitude to the thermal forces in our system. Additionally, we observe a temporal correlation between fluctuations in the radiation force and in the position of the resonator.

SCIENCE VOL 339 15 FEBRUARY 2013

